

Some Examples of Privacy-preserving Publication and Sharing of COVID-19 Pandemic Data

Fang Liu^{1*}, Dong Wang², Tian Yan¹

¹Department of Applied and Computational Mathematics and Statistics

University of Notre Dame, IN 46556, USA

²College of Cyberspace Security

Hangzhou Dianzi University, Wuhan, 430079, China

Abstract

A considerable amount of various types of data have been collected during the COVID-19 pandemic, the analysis and interpretation of which have been indispensable for curbing the spread of the disease. As the pandemic moves to an endemic state, the data collected during the pandemic will continue to be rich sources for further studying and understanding the impacts of the pandemic on various aspects of our society. On the other hand, naïve release and sharing of the information can be associated with serious privacy concerns. In this study, we use three common but distinct data types collected during the pandemic (case surveillance tabular data, case location data, and contact tracing networks) to illustrate the publication and sharing of granular information and individual-level pandemic data in a privacy-preserving manner. We leverage and build upon the concept of differential privacy to generate and release privacy-preserving data for each data type. We investigate the inferential utility of privacy-preserving information through simulation studies at different levels of privacy guarantees and demonstrate the approaches in real-life data. All the approaches employed in the study are straightforward to apply. Our study generates statistical evidence on the practical feasibility of sharing pandemic data with privacy guarantees and on how to balance the statistical utility of released information during this process.

keywords: COVID-19 pandemic, differential privacy, geo-indistinguishability, hot spot heat maps, contact tracing network, synthetic data

1 Introduction

A huge amount of data of various types have been collected during the COVID-19 pandemic, the analysis and interpretation of which has been indispensable to health authorities and experts to gain understanding of the disease, to identify risk factors, to monitor and forecast

*Corresponding author: Fang Liu (fang.Liu.131@nd.edu). Fang Liu was supported by NSF Grant NO. 1717417 and the University of Notre Dame Asia Research Collaboration Grant. Dong Wang was supported by the China Scholarships Council program (NO. 201906270230) and NSFC Grant NO. 41971407; Tian Yan was supported by the University of Notre Dame Asia Research Collaboration Grant and the Chinese Scholarship Council,

the spread of the disease, to evaluate the impacts of the pandemic on different aspects of our society, and to implement strategies that mitigates negative impacts. As the pandemic shifts to an endemic state, the collected data will continue to serve as rich sources for further research on the disease and its impacts so to prepare us for future pandemics.

Naïve release and sharing of the pandemic data can be associated with serious privacy concerns, especially considering that a huge amount and a great variety of data were collected quickly in a short period of time and the data privacy and ethics regulations were lagging behind at least in the initial stage of the pandemic. Many types of collected data are known to be associated with high privacy risk, such as disease status, medical history, locations, close contacts, employment/income status, etc. Balance must be found between individual privacy protection and sharing the data for research use.

Fortunately, this is not an unsolvable problem as many research questions of interest, the answers to which lie within the pandemic data, revolve around learning population-level and aggregate information rather than focusing on individual-level information which is often the goal of privacy attacks. If a privacy-preserving data release procedure can maintain accurate and useful aggregate information while guaranteeing individual-level privacy, it would make a potentially effective approach for data sharing.

Privacy-preserving collection and analysis of COVID-19 data have been developed and applied during the pandemic. Google research teams apply differential privacy (DP) to generate anonymized metrics from the data of Google users who opted in for the Location History setting in their Google accounts and produce the COVID-19 community mobility reports (Aktay et al., 2020), to understand the impacts of social distancing policies on mobility and COVID-19 case growth in the US (Wellenius et al., 2021), to generate anonymized trends in Google searches for COVID-19 symptoms and related topics (Fabrikant et al., 2020), and to forecast COVID-19 trends using spatio-temporal graph neural networks (Kapoor et al., 2020). DP is also integrated in deep learning to predict COVID-19 infections from imaging data (Müftüoğlu et al., 2020; Ulhaq and Burmeister, 2020). Butler et al. (2020) apply DP to generate individual-level health tokens/randomized health certificates while allowing useful aggregate risk estimates to be calculated. The methods in all the work above are designed to provide the usefulness of collective information in the released data without disclosing individual-level information upon release.

Location data and proximity data has been instrumental to track the trajectory of a COVID-19 case and for contact tracing (CT) so to identify people who might have close contacts with COVID-19 patients. On the other hand, location and relational information can be highly revealing of personal information in general. To protect the sensitive information, privacy-preserving technologies and tools are adopted in CT apps and software around the world during the pandemic to track the spread of the disease. The apps collect users' location data (e.g., GPS) or proximity data (e.g., Bluetooth), via either a centralized (e.g., Alipay Health Code and WeChat in China (Ghaffary, 2020), Corona100m in South Korea (Wray, 2020), COVIDTracker in Thailand (5Lab, 2020), ProteGo in Poland (Gad-Nowak and Grzelak, 2020), and Pan-European Privacy-Preserving Proximity Tracing (PEPP-PT) in EU (Parliament, 2020)) or decentralized model (Safe paths (Raskar et al., 2020) and the proximity-based Google/Apple Exposure Notification (GAEN) system (Apple and Google,

2020) in the US) to identify and notify those who might have been near a COVID-19 patient and at high risk of contracting the disease. We refer readers to Wang and Liu (2020) for a compensate review of the CT apps used during the pandemic.

Many privacy-preserving methods developed and implemented during the pandemic, including the work reviewed above, focus on information shared with governments, health officials, and the public so to facilitate quick decision making and timely actions during the pandemic. In contrast, privacy-preserving COVID-19 data release for research use has received less attention, which is the major focus of our work. Sharing data for research use is not just for making scientific discoveries, but also for producing real-world evidence and generating new insights into how we can better handle similar crisis in the future. Data for research use often contain granular information compared to those shared with administrators, decision makers, and the public, and thus are associated with higher privacy risk that must be mitigated before release.

We leverage and build upon existing DP concepts and techniques and apply them to several common but distinct pandemic data types to publish data with formal privacy guarantees. It is not our goal to cover all types of data collected during the pandemic, but rather use three pandemic data types – surveillance data, case location data, and contact tracing networks (CTNs) – to demonstrate how to apply formal privacy concepts to release privacy-preserving information. We choose the three data types because they data routinely collected during the pandemic, they are distinct in terms of data structure and statistical analysis, and they provide different information on COVID-19. Specifically, surveillance data help better understand risk factors associated with COVID-19 and identify sub-populations that are vulnerable to the disease; location data can be used to explore relationships between hot spots and residential characteristics to study issues such as residential racism and structural segregation during the pandemic, CTNs allow us to study how clustering of COVID-19 cases and how physical proximity may affect the spread of the disease, among others.

In all three data types, we focus on release of synthetic data generated at a pre-specified privacy budget. With synthetic data, data users may perform analysis on their own (Bowen and Liu, 2020). For surveillance data, we use the flat Laplace sanitizer with DP guarantees and examine statistical utility of log-linear models based on sanitized data, as a function of sample size and pre-specified privacy budget in simulation studies and real data published by the U.S. CDC. For location data, we apply the planar Laplace mechanism with geo-indistinguishability guarantees to release data. We conduct simulation studies and apply the method to a real South Korean case location dataset to examine inference from cluster point process models and accuracy of hot spot heat maps based on sanitized locations. For CTN data, we examine the feasibility of the approach of differentially private exponential random graph models (ERGMs) to generate privacy-preserving synthetic networks. We conduct simulation studies to investigate the utility of sanitized networks in inference from ERGMs and preservation of descriptive structural network information.

The rest of the paper is organized as follows. Section 2 provides an overview of the basic concepts in DP, some common randomized mechanisms for achieving DP, and an approach for obtaining valid inferences from sanitized data. Section 3, 4 and 5 apply DP procedures to release privacy-preserving case surveillance data, case location data, and CTNs, respectively,

conduct simulation studies to examine the statistical utility of the privacy-preserving data, and apply the DP procedures to real pandemic data. Section 6 provides some final remarks on the implementations of DP methods in releasing COVID-19 data.

2 Preliminaries

We provide a brief overview of some common DP concepts and mechanisms. The overview is not comprehensive and does not aim at covering every concept in DP, but rather focuses on those used or mentioned in this paper.

2.1 Differential privacy

Definition 1 ((ϵ, δ) -DP (Dwork et al., 2006a,b)). *A randomized algorithm \mathcal{M} is of (ϵ, δ) -DP if for all dataset pairs of neighboring data sets (D, D') differing by one record and for all subsets $\mathcal{S} \subseteq \text{image}(\mathcal{M})$,*

$$\Pr(\mathcal{M}(D) \in \mathcal{S}) \leq e^\epsilon \Pr(\mathcal{M}(D') \in \mathcal{S}) + \delta. \quad (1)$$

D and D' differing by one record (denoted by $d(D, D') = 1$) may refer to the case that they are of the same size but differ in at least one attribute value in exactly one record (bounded DP), or D' has one record less than D or vice versa (unbounded DP) (Kifer and Machanavajjhala, 2011). $\epsilon > 0$ and $\delta \geq 0$ are privacy budget or privacy loss parameters. When $\delta = 0$, (ϵ, δ) -DP becomes pure ϵ -DP; the smaller ϵ is, the more privacy protection there is on any individual in the data, as the released results $\mathcal{M}(D)$ and $\mathcal{M}(D')$ are similar in the sense that their probability density/mass function ratio is bounded with $(e^{-\epsilon}, e^\epsilon)$. There is no consensus and lacks a universal guideline on the choice of ϵ (Dwork et al., 2019). ϵ typically ranges from 10^{-3} to 10 in empirical studies in the DP literature on, depending on the type of information released, social perception of privacy, expected accuracy of released data, among others. Real-life of applications of DP often employs larger ϵ for better utility (e.g., US Census uses ϵ of 19.61 (Bureau, 2020) and Apple Inc. sets ϵ at 2, 4, or 8 for different Apps (Apple, 2020)). δ , if not 0, is often set at a very small value (inverse proportional to $\text{poly}(n)$) and can be interpreted as the probability that the pure ϵ -DP is violated.

Definition 1 is the original DP definition. Relaxed versions and extensions exist, such as (ϵ, δ) -probabilistic DP (pDP) (Machanavajjhala et al., 2008), (ϵ, τ) -concentrated DP (CDP) (Dwork and Rothblum, 2016), zero-concentrated DP (Bun and Steinke, 2016) (zCDP), Rényi DP (RDP) (Mironov, 2017), and Gaussian DP (GDP) (Dong et al., 2021).

DP provides a mathematically rigorous framework for protecting individual privacy when releasing and sharing information. Many mechanisms and procedures have been developed to achieve DP. In this paper, we employ the Laplace mechanism with pure ϵ -DP to illustrate how to apply DP concepts and procedures to protect individual privacy when releasing COVID-19 data. When other types of DP guarantees are desired, such as (ϵ, δ) -(p)DP, corresponding mechanisms can be used, such as the Gaussian mechanisms (Dwork and Roth, 2014; Liu, 2018).

Definition 2 (Laplace mechanism (Dwork et al., 2006b)). *Let $\mathbf{s} = (s_1, \dots, s_r)$ be a statistic calculated from a dataset. The Laplace mechanism of ϵ -DP releases $\mathbf{s}^* = \mathbf{s} + \mathbf{e}$, where \mathbf{e} contains r independent samples from $\text{Laplace}(0, \Delta\epsilon^{-1})$, where $\Delta_1 = \max_{x, x', d(x, x')=1} \|\mathbf{s}(x) -$*

$\mathbf{s}(x')\|_1$ is the ℓ_1 global sensitivity of \mathbf{s} .

The ℓ_1 global sensitivity represents the maximum ℓ_1 change in \mathbf{s} between two neighboring data sets (in general, one can define ℓ_p ($p \geq 0$) global sensitivity; see Liu (2018)). The larger the sensitivity, the more impact a single individual has on the value of \mathbf{s} and more noise would be needed to achieve ϵ -DP.

Every time a dataset is queried, there is a privacy cost (loss) on the individuals in the dataset. Data curators need to track the privacy cost during the querying process to ensure the overall privacy spending does not exceed a pre-specified level. Two basic composition principles in DP, *parallel composition* and *sequential composition* (McSherry and Talwar, 2007), can be used in privacy loss accounting, which are also used in later sections of the paper.

Definition 3 (Basic privacy loss composition (McSherry and Talwar, 2007)). *If mechanism \mathcal{M}_j of (ϵ_j, δ_j) -DP is applied to disjoint dataset D_j for $j = 1, \dots, P$, the parallel composition states the total privacy loss in data $\cup_j D_j$ from apply the P mechanisms \mathcal{M}_j for $j = 1, \dots, P$ is $(\max\{\epsilon_j\}, \max\{\delta_j\})$; if \mathcal{M}_j is applied to the same dataset D , the sequential composition states that the total privacy loss in D is $(\sum_j \epsilon_j, \sum_j \delta_j)$ from applying the P mechanisms \mathcal{M}_j for $j = 1, \dots, P$.*

In layman’s terms, the two privacy loss composition principle states as long as there is no overlapping information between two datasets to which two DP mechanisms is applied to, the overall loss for releasing the queries results is the maximum privacy spending between the two; otherwise, the loss adds up. The sequential composition on (ϵ, δ) -DP can be over-conservative for repeated querying on the same data; advanced composition (Dwork et al., 2010) for (ϵ, δ) -DP and the relaxed DP notions mentioned above (e.g., CDP, zCDP, RDP, GDP) all achieve tighter total privacy loss bound than the basic composition.

DP is a main-stream concept in privacy research and applications nowadays. Backed up its mathematical rigor and robustness to various privacy attacks, the properties it has, including privacy loss composition, immunity to post-processing, and being future-proof, make it attractive for designing sophisticated DP procedures and algorithms for complicated analysis and learning problems such as deep learning (Abadi et al., 2016) and regularized regressions (Chaudhuri et al., 2011; Kifer et al., 2012; Li and Liu, 2022). Immunity to post-processing and being future-proof refer to instances that information released from a DP mechanism won’t leak additional information about the individuals in the dataset on which the information is based when it is further processed after the release or when there is additional information on these individuals in the future from other sources, as long as the original data is not accessed.

2.2 Location privacy

Andrés et al. (2013) extend the pure ϵ -DP concept to releasing privacy-preserving location data that are represented as pairs of 2-dimensional GPS coordinates, along with the planar Laplace mechanism to achieve such privacy guarantees.

Definition 4 (Geo-indistinguishability (GI) (Andrés et al., 2013)). *Let $d(P, P')$ denote the Euclidean distance between any two distinct locations P and P' , and ϵ be the*

unit-distance privacy loss. A randomized mechanism \mathcal{M} satisfies ϵ -GI if and only, for any $\gamma > 0$, any possible released location P^ , and all possible pairs of P and P' that $d(P, P') \leq \gamma$,*

$$\Pr(\mathcal{M}(P) = P^* | P) \leq e^{\epsilon\gamma} \cdot \Pr(\mathcal{M}(P') = P^* | P'). \quad (2)$$

\mathcal{M} in Eq (2) enjoys $(\epsilon\gamma)$ -GI for any specified $\gamma > 0$ in the sense that the probability of distinguishing any two locations within a radius of γ , given the released location P^* , is $e^{\epsilon\gamma}$ -fold the probability when not having P^* . ϵ is the per-unit-distance loss and γ denotes how many units. The larger ϵ is, the larger the privacy loss ($\epsilon\gamma$) is and the higher probability of identifying the true location information within a radius of γ mile given the perturbed location information. Though increasing γ would also lead to higher privacy loss and probability identifying the true location is within a radius of γ but the large γ would make this identification less meaningful.

Definition 5 (planar Laplace mechanism (Andrés et al., 2013)). *Let the coordinates of the observed location P in the Euclidean space be (x, y) . The planar Laplace mechanism of ϵ -GI generates sanitized location P^* with coordinates*

$$(x^*, y^*) = (x + r \cos(\theta), y + r \sin(\theta)), \text{ where} \quad (3)$$

$$r \sim \text{gamma}(2, \epsilon) = r\epsilon^2 e^{-\epsilon r} \text{ and } \theta \sim \text{uniform}(0, 2\pi) = 1/(2\pi). \quad (4)$$

r in Eqs (4) is the distance between P^* and P and θ is the angle of $P \rightarrow P^*$ in the Euclidean space, and r and θ are independent. The concepts of GI and planar Laplace mechanism are employed in Section 4 for releasing privacy-preserving location data.

More precisely speaking, GI is more related to local DP (Duchi et al., 2013), an extension of the pure ϵ -DP, than the latter per se, which is often used for releasing aggregate information rather than individual response.

Definition 6 (ϵ -local DP (Duchi et al., 2013)). *A randomization mechanism \mathcal{M} provides ϵ local DP if $\Pr[\mathcal{M}(x) \in \Omega] \leq e^\epsilon \cdot \Pr[\mathcal{M}(x') \in \Omega]$ for all pairs of possible data points x and x' from an individual and all possible output subset Ω from \mathcal{M} .*

2.3 Privacy-preserving statistical inference

Sanitized outputs, compared to the original outputs, are subject to an extra source of variability due to the noise introduced through the randomized algorithm \mathcal{R} for achieving DP. To account for the extra source of variability for valid statistical inference, one may directly model the sanitization mechanism, which may complicate the regular inferential procedures either analytically or computationally and is problem-specific. An alternative is the multiple synthesis (MS) approach that releases multiple sets of sanitized datasets or statistics and employs an inferential rule across the multiple sets to obtain valid inference Liu (2022). The MS approach is general and straightforward to apply. We adopt the MS approach to obtain privacy-preserving inference from sanitized data in this paper.

Denote the number of released sets by m . Per sequential composition, the total privacy budget would split into m portions, one per release. $m \in [3, 5]$ is recommended (Liu, 2022). WLOS, suppose the parameter of interest is β and its l -th sanitized estimate is $\hat{\beta}^{(l)}$ with estimated variance $w^{(l)}$ for $l = 1, \dots, m$. The final inference of β , including hypothesis

testing and confidence interval (CI) construction, is based on the following inferential rule.

$$\bar{\beta} = m^{-1} \sum_{l=1}^m \hat{\beta}^{(l)}, \quad T = m^{-1}B + W \quad (5)$$

$$(\beta - \bar{\beta})T^{-1/2} \sim t_{\nu=(m-1)(1+mW/B)^2}, \quad \text{where} \quad (6)$$

$$B = \sum_{l=1}^m (\hat{\beta}^{(l)} - \bar{\beta})^2 / (m - 1) \quad (\text{between-set variability})$$

$$W = m^{-1} \sum_{l=1}^m w^{(l)} \quad (\text{within-set variability}).$$

3 Privacy-preserving Case Surveillance Data Release

We present privacy-preserving release of three pandemic data types: subgroup case surveillance data (Section 3), case location data (Section 4), and CTNs (Section 5). In each case, we describe data characteristics, introduce methods for sanitization, conduct a simulation study to examine the impact of sanitization on statistical inference, and apply the method to a real data set when one is available.

Case surveillance data are listing of cases, together with attributes associated with the cases, such as demographics, exposure histories, etc. Surveillance data are crucial during the pandemic for monitoring and forecasting the spread of the disease, understand how COVID impacts the capacity of healthcare systems, and provide necessary information to health authorities for quick decision making. Case numbers reported at different geographical scales by demographic groups such as age, gender, race and ethnicity provide valuable information for identifying risk factors and groups vulnerable to the disease and understanding the heterogeneity of the susceptibility to the disease. On the other hand, publishing such granular information may lead to re-identification and disclosure risk, especially when data are sparse. This section focuses on publishing granular case numbers with privacy guarantees.

An example of case surveillance data is the COVID-19 death count data released by the U.S. CDC website. Table 1 show such a dataset we downloaded on May 24, 2022 (Table 2 at https://www.cdc.gov/nchs/nvss/vsrr/covid19/health_disparities.htm) with some minor modifications (we removed the race group ‘unknown’ and collapsed age groups (0, 4] and [5, 17] to a single < 18 group, and age groups [75, 84] and ≥ 85 to a single > 74 group). Table 1 contains two attributes – age group and race/ethnicity; each has 7 levels, leading to a 7 × 7 contingency table. The sample size $n = 998,262$, assumed to be public information.

Table 1: U.S. COVID-19 death counts by age and race/ethnicity (May 24, 2022)

Age (ys) group	Race/Ethnicity							Total
	NH White	NH Black	NH AIAN	NH Asian	NH NHPI	NH Mix	Hispanic	
<17	387	274	15	36	11	30	303	1056
18-29	2263	1492	187	190	49	73	2015	6269
30-39	6661	4144	560	558	151	157	5919	18150
40-49	17269	8937	1021	1206	265	309	13981	42988
50-64	97418	35753	3198	5312	715	952	43657	187005
65-74	141409	37765	2901	7423	501	913	38422	229334
>75	380630	54576	3210	16504	449	1380	56711	513460
Total	646037	142941	11092	31229	2141	3814	161008	998262

Race/ethnicity = ‘unknown’ is not included in the table.

NH = Non-Hispanic; AIAN = American Indian or Alaska Native; NHPI = Native Hawaiian or Other Pacific Islander; ‘Mix’ means ‘more than one race’

3.1 Method

Publishing a privacy-preserving case number dataset can be formulated as releasing a multi-dimensional histogram or contingency table. The most straightforward approach for achieving DP when releasing a histogram and contingency table is the flat Laplace sanitizer, which injects noise from the Laplace mechanism directly into each cell count in a histogram or contingency table; methods that achieve better utility in sanitizing count data for certain analyses exist, at the cost of more complicated implementation, such as Bowen et al. (2021); Eugenio and Liu (2021); Geng and Viswanath (2015); Hay et al. (2010); Li et al. (2018); Xiao et al. (2011, 2012); Xu et al. (2013); Zhang et al. (2014), just to name a few. Given that there exist many methods for sanitizing count data, many aiming at improving the utility of a certain type of analysis and not straightforward to implement, and our main goal is to demonstrate the application of DP in releasing count data in general without a specific downstream analysis task in mind, we employ the flat Laplace mechanism (we examined a couple of other approaches, but their performance is not as good as Laplace sanitizer in the in utility analysis. More details are provided in Section 3.4).

In our problem setting, the Laplace sanitizer employs the Laplace mechanism in Definition 2 to sanitize each cell count of the multidimensional histogram/ contingency table to be released. The l_1 global sensitivity of releasing a histogram/table is 1 (WLOS, we use the unbounded DP unless mentioned otherwise; the sensitivity is 2 if the bounded DP is used). Sanitized count in cell k is $\tilde{y}_k \sim \text{Laplace}(y_k, \epsilon^{-1})$ for $k = 1, \dots, K$ cells. Sanitized counts may be negative as the support of the Laplace distribution is the real line. There are two ways to deal with this problem – to replace negative values by 0, and to re-draw until the sanitized value is non-negative (Liu, 2019). In either case, normalization would be needed if the total sample size n is fixed. Real non-negative sanitized counts can be rounded to obtain integer counts without compromising privacy due to the immunity to post-processing property.

To obtain sanitized counts for a lower-dimensional histogram/contingency table from the sanitized histogram/table at a more granular level, one may sum sanitized counts over corresponding cells to obtain cells counts in the lower-dimensional histogram/table. Per the immunity to post processing property, the summed counts are also privacy-preserving, but are subject to a larger sanitization variability since each contains the sum of multiple independent noise terms.

3.2 Simulation Study

We use a simulation study to study how DP sanitization affects statistical inference based on sanitized count data. We simulated 1,000 datasets from $y_k \sim \text{multinomial}(n, p_k)$, where $p_k = \lambda_k / (1 + \lambda_k)$, $\log(\lambda_k) = \beta_0 + \beta_1 x_{k1} + \beta_2 x_{k2} + \beta_3 x_{k3} + \beta_4 x_{k1} x_{k2} + \beta_5 x_{k1} x_{k3} + \beta_6 x_{k2} x_{k3}$ for $k = 1, \dots, 8$ and $X_1 = \{0, 1\}$, $X_2 = \{0, 1\}$, $X_3 = \{0, 1\}$ are binary attributes. In each dataset, we sanitize $\mathbf{y} = \{y\}_{k=1, \dots, 8}$ via the flat Laplace sanitizer independently for $m = 3$ times to obtain differentially private $\tilde{\mathbf{y}}^{(l)}$ and $l = 1, \dots, m$, each at a privacy budget of ϵ/m , where ϵ is the total privacy budget. We examine two sample sizes at $n = 200$ and $n = 1,000$ and four privacy loss parameters at $\epsilon = 0.5, 1, 2$ and 5 . We assume the total sample size n is fixed and normalize the raw sanitized counts from the flat sanitizer via $n\tilde{y}_k^{(l)} / \sum_l \tilde{y}_k^{(l)}$. For utility check, we run the loglinear model $\log(\lambda_k) = \beta_0 + \beta_1 x_{k1} + \beta_2 x_{k2} + \beta_3 x_{k3} + \beta_4 x_{k1} x_{k2} + \beta_5 x_{k1} x_{k3} + \beta_6 x_{k2} x_{k3}$

for $k = 1, \dots, 8$, assuming $\tilde{\mathbf{y}}_k^{(l)} \sim \text{Poisson}(\lambda_k)$, on each set of sanitized data to obtain inference on β_1, \dots, β_6 using Eqs (5) and (6). For comparison, we also run the same loglinear model on the original \mathbf{y} .

The results are presented in Figure 1 and the main observations are summarized as follows. The smaller ϵ or n is, the more impact the DP procedure has on the inference; i.e., larger bias and larger root mean squared error (RMSE). Regardless of n or ϵ , the coverage probability (CP) of the 95% CIs is always at the nominal level. At $n = 1,000$, the inference is barely affected by the DP sanitization even for $\epsilon = 0.5$. At $n = 200$, the bias is noticeable with relatively large RMSE for $\epsilon = 0.5$, acceptable at $\epsilon = 1$, and almost ignoble for $\epsilon > 1$, compared to the original inference.

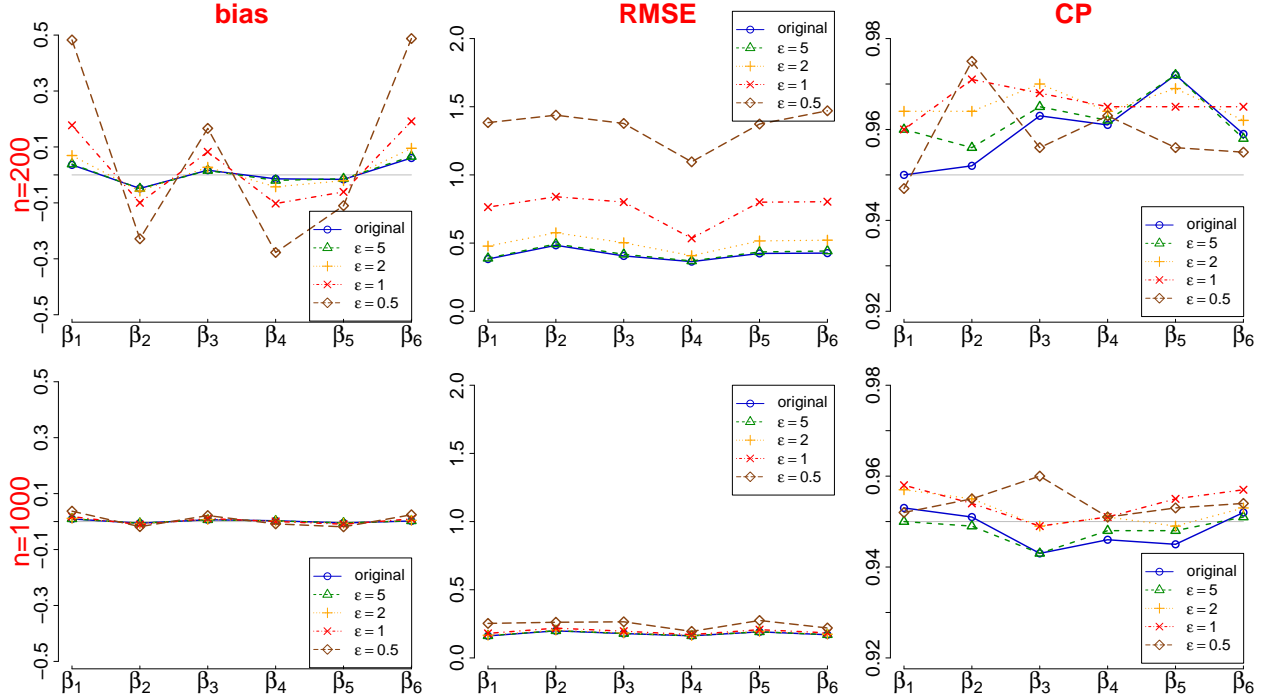


Figure 1: Privacy-preserving inference in log-linear model on sanitized counts obtained via the flat Laplace sanitizer in simulated data (1000 repeats)

3.3 Application to CDC case surveillance data

We apply the flat Laplace sanitizer to the CDC in Table 1. If released data are not used for statistical inference or uncertainty quantification, we may release a single sanitized tabular dataset ($m = 1$). Let $\tilde{y}_k = y_k + e_k$, where $e_k \sim \text{Laplace}(0, \epsilon^{-1})$, for $k = 1, \dots, 49$ independently. Since $n = 998,262$ is public knowledge, the sanitized \tilde{y}_k is normalized as in $\tilde{y}_k \leftarrow n\tilde{y}_k / \sum_k \tilde{y}_k$ to keep the total n at 998,262. An example sanitized dataset at $\epsilon = 0.5$ is given in Table 2. There is some fluctuation in each cell count due to the sanitization, as expected. The column and row marginals are calculated by summing over the corresponding cell counts after sanitization.

If the data will be used for statistical inference, we can use the MS approach to release multiple sets of sanitized tables. We set $m = 3$ and sanitized y_k with noise from $\text{Laplace}(0, \epsilon/m)$ independently to obtain 3 sets of sanitized $\tilde{y}_k^{(l)}$ for $l = 1, 2, 3$. Some example sanitized data

Table 2: Flat Laplace sanitized ($\epsilon = 0.5, m = 1$) US COVID-19 death counts by age group and race/ethnicity on May 24, 2022

Age (ys) group	Race/Ethnicity							Total
	NH White	NH Black	NH AIAN	NH Asian	NH NHPI	NH Mix	Hispanic	
<17	385	271	14	37	8	29	308	1052
18-29	2258	1491	186	198	49	72	2009	6263
30-39	6664	4140	562	558	145	156	5928	18153
40-49	17269	8937	1021	1202	266	299	13982	42976
50-64	97421	35753	3195	5311	713	952	43658	187003
65-74	141413	37766	2897	7427	501	914	38425	229343
>75	380642	54577	3209	16505	449	1379	56712	513472
Total	646053	142935	11084	31238	2130	3801	161021	998262

Race/ethnicity = 'unknown' is not included in the table.

NH = Non-Hispanic; AIAN = American Indian or Alaska Native; NHPI = Native Hawaiian or Other Pacific Islander; "Mix" means "more than one race"

are provided in the supplementary materials. For the statistical analysis on the sanitized data, we fitted a 2-way loglinear model with covariates age group and race/ethnicity (other analysis can also be run, such as logistic regression, Chi-squared test). There are 48 regression coefficients – 6 associated with age (< 18 years is the reference group), 6 associated with race (non-Hispanic white is the reference group), and 36 parameters representing the interaction between the two. The estimates of the regression coefficients are presented in Figure 2. In summary, the privacy-preserving inferences based on the sanitized counts are similar to the original inference at all ϵ values, largely due to the large sample size of the data.

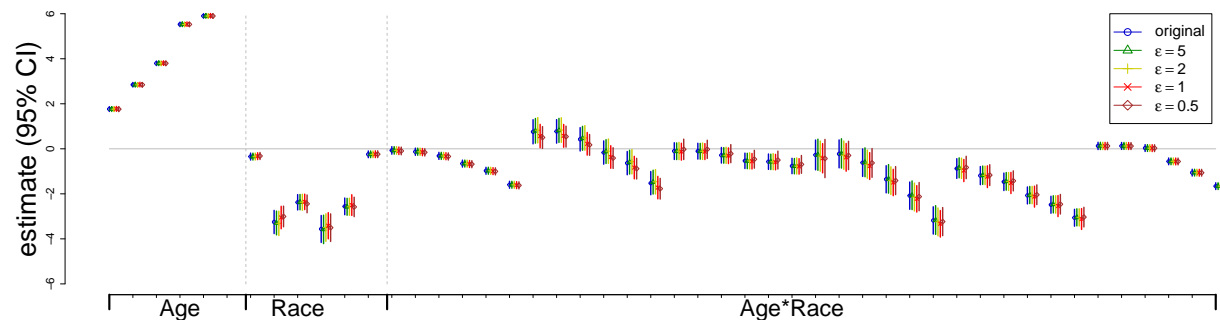


Figure 2: Privacy-preserving results from the log-linear model on sanitized CDC COVID-19 death data via the flat Laplace sanitizer

3.4 Summary

Case number data with granular information permits more complicated analysis and helps us understand better the pandemic, such as quantifying the effects of risk factors for COVID-19 as demonstrated in Figure 2). We demonstrate via a simulation study and a real data application that useful privacy-preserving can be achieved, especially when n is large or people are willing to sacrifice some privacy (ϵ is not too small). The results also suggest the flat Laplace sanitizer can be an effective approach for that purpose, despite its simplicity.

Though we focus on the flat Laplace sanitizer for demonstration purposes, we also run a couple of other methods that sanitize count data in a hierarchical manner in the simulation

study and the case study. The two approaches are – the universal histogram (UH) approach (Hay et al., 2010) and its extension UH-proportion or simply UHp that we extend UH for the case where the total sample size of the released data is fixed and public. The descriptions of the UH and UHp approaches, the details of their implementation, and the results from the simulation study and the case study are presented in the supplementary materials. In summary, UHp delivers comparable performance to the flat sanitizer in bias and RMSE for most of the parameters in the simulation study, but has slight under-coverage at $\epsilon = 1$ and 0.5. UH performs the worst (largest bias, RMSE, and some notable under-coverage). In the case study, there is some discrepancy between the privacy-preserving point estimates vs the original for both UH and UHp. For UH, some CIs are noticeably wider than the original, mostly in the race/ethnicity groups that are relatively small in size.

4 Privacy-preserving Release of Case Location Data

When a person is diagnosed with COVID-19, health authorities may interview the person for his or her whereabouts and location history in the past few weeks (CDC, 2021; National Health Commission of China, 2021b). Patient’s location data are critical for health authorities to take measures to limit the spread of the disease. With individual-level location data, researchers can conduct spatial data analysis such as using point process models to understand the spatial trend of the cases or generating COVID-19 hot spot heat maps. However, location information, if shared as is, may cause serious privacy risk for the patients and can even lead to cyber-bullying (National Health Commission of China, 2021a).

We examine a privacy-preserving approach to releasing location data based on GI. We focus on releasing cross-sectional location data at a given time point rather than travel trajectories Liu et al. (2021), which is a topic for future research. Even though released data is cross-sectional, they can be released on a regular time basis, e.g., every day or every 3 days, allowing temporal examination of certain trends.

An example of location data is given in Figure 3, which shows the locations of 121 COVID-19 patients on Feb 20, 2020 in South Korea. The data can be found in file “patientroute.csv” at <https://www.heywhale.com/mw/dataset/5e797e9e98d4a8002d2c92d3/file>. The number of locations per subject ranges from 1 to 11; about 50% (62 out of 121) has one location, 34.7% has 2 or 3 locations, and the rest 14% have ≥ 4 locations (one person has 11 locations; all within the city of Gwangju). The timestamp information in hours, minutes, and dates is not available in the dataset.

4.1 Method

The approach we propose for releasing privacy-preserving location information is *the doppelganger* Liu et al. (2021), based on the GI concept. The main idea behind doppelganger, as suggested by the name, is to release $m \geq 1$ sanitized versions of the true location P via the planar Laplace mechanism so to satisfy GI guarantees. The privacy budget per location ϵ is split into m portion for $m \geq 2$, ϵ/m per release. Similar to case surveillance data, the main reason for releasing multiple perturbed locations ($m \geq 2$) is to provide a way to quantify sanitization uncertainty and draw statistical inferences using the MS approach.

To generate a sanitized location (x^*, y^*) given the original location coordinates (x, y) , we

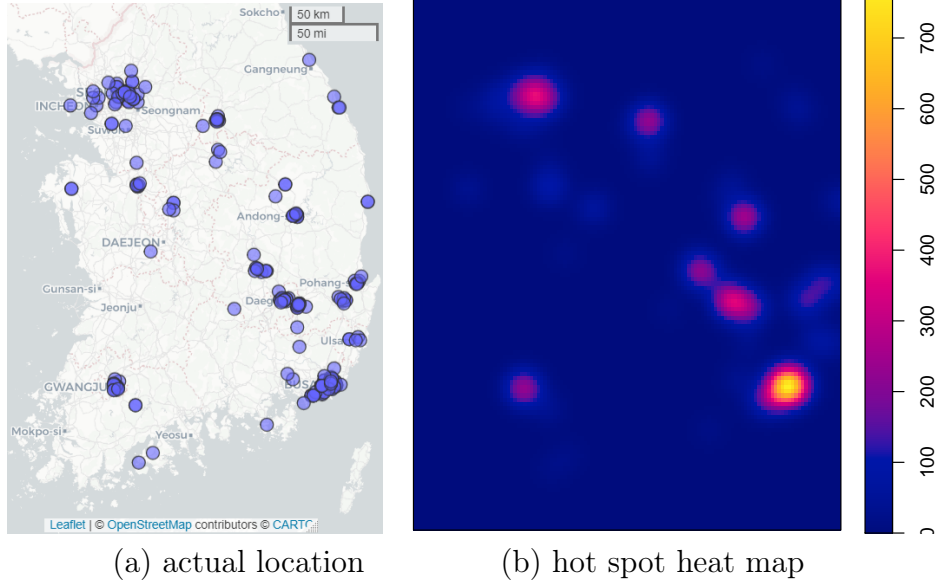


Figure 3: Locations of 121 COVID-19 patients on Feb 20, 2020 in South Korea

apply the planar Laplace mechanism in Eq (3), with ϵ replaced by ϵ/m . ϵ is the per-unit-distance privacy loss, where the unit distance is supplied by the data curator and can be any value deemed appropriate for the task at hand, such as 1 meter, 10 meters, 0.5 miles, etc (generally speaking, the choice depends on location type, area, among other considerations).

4.2 Simulation Study

To evaluate statistical utility of sanitized locations via doppelganger, we conduct a simulation study. We simulated 1,000 sets of location data in a square area of $[0, 1] \times [0, 1]$ from an inhomogeneous Matérn cluster point process with the radius of the clusters at 0.03 and the non-stationary log-density $\log(\lambda(x, y; \beta)) = \beta_0 + \beta_1 x + \beta_2 y + \beta_3 x^2 + \beta_4 y^2 + \beta_5 xy$, where x and y are coordinates and $\beta = (\beta_0, \dots, \beta_5) = (4.53, 3.30, 3.43, -0.27, 1.58, 2.24)$. The number of locations ranges from 769 to 1217 across the 1,000 repeats with an average of 970. In each simulated dataset, we sanitized each location with the planar Laplace mechanism in Eq (3) at $\epsilon = 5, 2, 1, 0.5$ per 0.01 unit and $m = 3$. We assume $[0, 1] \times [0, 1]$ is public information and sanitized locations thus should fall within $[0, 1] \times [0, 1]$. On the other hand, the planar Laplace mechanism can generate an infinite r and any angle $\in [0, 2\pi]$. To honor the location boundaries, we set sanitized $x^* < 0$ at 0 and at 1 if it is > 1 ; similarly for sanitized y^* . We then fitted the inhomogeneous Matérn cluster point process model above and applied the inferential rule in Eq (6) to obtain inference on β . The data simulation and analysis were conducted using R package `spatstat.core` (Baddeley and Turner, 2005).

The results are presented in Table 3. In summary, the inferences at $\epsilon = 5$ and $\epsilon = 2$ are comparable to the original – close-to-0 bias, similar RMSE as the original, nominal converge at $\epsilon = 5$ and slight under-coverage at $\epsilon = 2$. At $\epsilon = 1$ and $\epsilon = 0.5$, the bias is notable; the RMSE values are similar to the original at $\epsilon = 1$, but much larger at $\epsilon = 0.5$; the CP is around 83% to 85% at $\epsilon = 1$ and ranges from 60% to 88% at $\epsilon = 0.5$. The moderate to severe under-coverage is largely due to the bias in the β estimates, which in turn may be attributed to the bounding applied to the sanitized locations. Bounding sanitized values can lead to biased inference (Liu, 2019).

Table 3: Privacy-preserving inferences of Matérn cluster point process model on simulated location data (1,000 repeats, $m = 3$)

metric	parameter	original	$\epsilon = 5$	$\epsilon = 2$	$\epsilon = 1$	$\epsilon = 0.5$
bias	β_0	-0.029	-0.022	0.016	0.142	0.571
	β_1	0.065	0.052	-0.022	-0.279	-1.180
	β_2	0.031	0.014	-0.074	-0.374	-1.389
	β_3	-0.085	-0.077	-0.028	0.154	0.801
	β_4	0.034	0.038	0.060	0.124	0.337
	β_5	-0.037	-0.024	0.048	0.303	1.160
RMSE	β_0	0.466	0.465	0.459	0.457	0.680
	β_1	1.234	1.232	1.211	1.189	1.549
	β_2	1.164	1.162	1.152	1.166	1.693
	β_3	1.006	1.003	0.986	0.958	1.159
	β_4	0.944	0.943	0.934	0.898	0.838
	β_5	0.985	0.982	0.972	0.989	1.431
CP	β_0	0.948	0.940	0.925	0.841	0.599
	β_1	0.938	0.932	0.914	0.845	0.719
	β_2	0.957	0.952	0.935	0.851	0.640
	β_3	0.938	0.929	0.909	0.842	0.769
	β_4	0.941	0.934	0.908	0.840	0.878
	β_5	0.947	0.939	0.916	0.827	0.638

4.3 Application to South Korea case location data

We apply the doppelganger to the real South Korean case location dataset (Figure 3(a)) to release privacy-preserving locations at $\epsilon = 5, 2, 1, 0.1$ per 2 miles per individual. For an individual who has more than one location record, we further divided ϵ by the number of locations for that individual. That is, if an individual has h original location data points and we release m sanitized locations for each location at a privacy budget of $\epsilon/(mh)$. Similar to the simulation study, we honor the fact that all cases are in South Korea and bounded sanitized locations within a rectangular that approximates the shape of South Korea, in a similar fashion as done in the simulation study.

We used two analyses to check the utility of the sanitized locations: to generate hot spot heat maps and to fit a point process model. We set $m = 3$ in both analyses but also examined $m = 1$ in the former as it does not involve statistical inference. The privacy-preserving heat maps are displayed in Figure 4 with the same smoothing bandwidth as in Figure 3(b). The privacy-preserving hot spot heat maps are very similar to the original heat map in Figure 3(b) at $\epsilon \geq 1$ for both $m = 1$ and $m = 3$ and are a bit noisy at $\epsilon = 0.5$ especially when $m = 3$; but the major hot spots (the cities of Busan, Seoul, and Daegu) are preserved at $\epsilon = 0.5$ for $m = 1$. In summary, for the purposes of generating heat maps, $m = 1$ is sufficient and each sanitized location is less noisy compared to using $m = 3$ especially at small ϵ .

We fitted an inhomogeneous Matérn cluster point process model with log-density $\log(\lambda(x, y; \boldsymbol{\beta})) = \beta_0 + \beta_1 x + \beta_2 y$ on the original data and the sanitized data. For this analysis, we randomly selected one location if an individual has multiple original location records, resulting in one original location per individual. We applied the inferential rule in Eqs (5) and (6) to obtain the point estimates and 95% CIs for $(\beta_0, \beta_1, \beta_2)$. The results are presented in Table

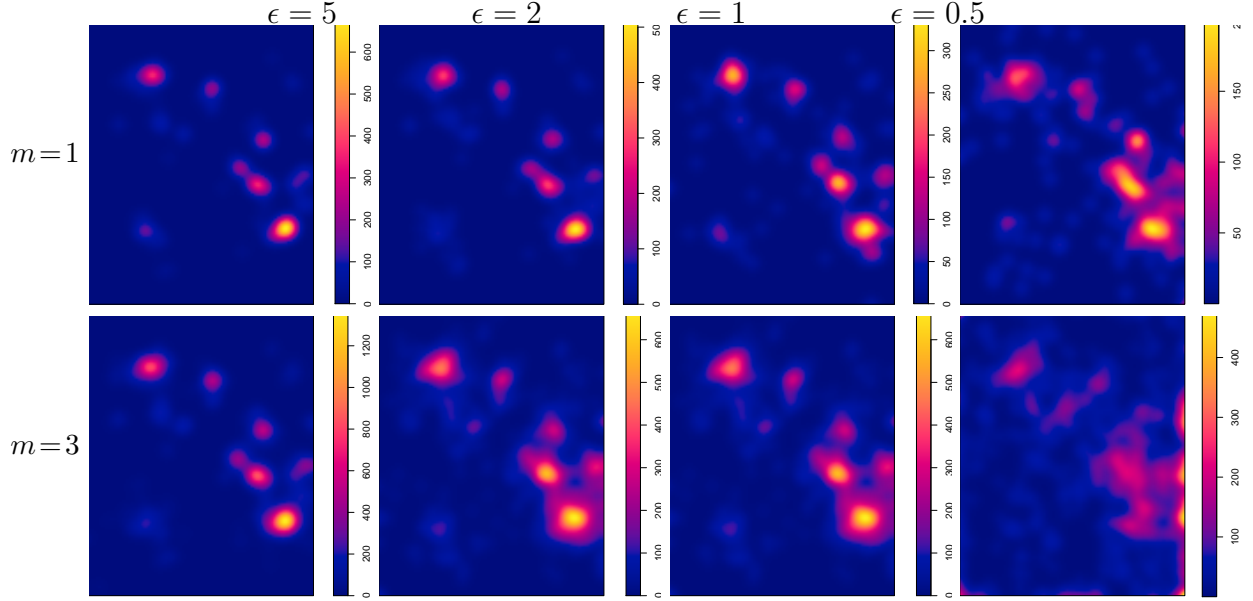


Figure 4: Privacy-preserving COVID-19 hot spot heat maps in South Korea on Feb 20, 2020

4. In general, the privacy-preserving inferences are similar to the original, especially for β_1 and β_2 that quantify the linear trends of COVID intensity along the x and y coordinates, respectively. In addition, the privacy-preserving point estimates are robust to $\epsilon \geq 1$ and some notable deviation from the original is only seen at $\epsilon = 0.5$. A surprising observation is the shrinkage in the CIs as ϵ decreases for $\epsilon < 5$, implying the inferences become more precise, at least for the range of the examined ϵ values, though the statistical insignificance remains unchanged across ϵ . The shrinkage is counter-intuitive as one would expect the inferences get less precise as the locations are perturbed more at smaller ϵ . As ϵ decreases, the sanitized locations are more scattered (Figure 4) and the likelihood of a sanitized location being bounded at the boundary also increases, which may affect the within and between components of the total variance in Eq (5). More research is needed to understand precisely how the variability is affected by the sanitization and the bounding constraint.

Table 4: Privacy-preserving Matérn cluster point process model parameter estimates based on sanitized locations in the South Korea location data ($m=3$).

	estimate (95% CI)				
	original	$\epsilon = 5$	$\epsilon = 2$	$\epsilon = 1$	$\epsilon = 0.5$
β_0	-64.2 (-153.5, 25.1)	-65.1 (-157.0, 26.9)	-63.0 (-147.0, 21.0)	-63.8 (-140.6, 13.0)	-57.5 (-129.8, 14.7)
β_1	0.51 (-0.17, 1.19)	0.52 (-0.18, 1.21)	0.50 (-0.14, 1.14)	0.50 (-0.08, 1.08)	0.44 (-0.10, 0.99)
β_2	0.03 (-0.50, 0.56)	0.03 (-0.52, 0.59)	0.03 (-0.48, 0.54)	0.05 (-0.42, 0.51)	0.07 (-0.39, 0.53)

4.4 Summary

The doppelganger method releases location data with privacy guarantees. The simulation study and the case study suggest the method can preserve important statistical signals in the original data at a relatively low-level cost of privacy. The method would be particularly useful for protecting location privacy when sharing information at a local level or releasing hot spot maps on a relatively fine scale. The finer the scale is, the more sparse the data become, the higher the privacy risk for re-identification from releasing location data, and the greater the need for effective privacy protection approaches, but also the noisier released

sanitized locations. As the scale gets coarser, say at the city, regional, state, or national levels, the information released by the doppelganger can be very similar to the original location information.

5 Privacy-preserving Sharing of Contact Tracing Networks (CTNs)

Contact tracing (CT) is an effective approach for curbing the spread of COVID-19 during the pandemic. CT can be carried out manually by human tracers or digitally via GPS or Bluetooth devices. CTNs, constructed from CT data, can be regarded as a type of social networks with individuals being the nodes and an edge between two people representing a close contact between them (e.g., within 6 feet of each other for a cumulative total of 15 minutes or more over a 24-hour period). CTNs are of research interest as they provide valuable information to better understand how physical proximity affects the spread of the disease and human contact behaviors during the pandemic, among others. However, sharing CTNs as is has privacy concerns as adversaries may link a CTN with other databases or use background knowledge to infer who were infected with COVID-19 and tell who were close physically (appearing in the same place at the same time) based on the edge information in a CTN.

CT data are only collected as needed – that is, when a person is diagnosed positive for COVID-19. Therefore, a CTN only contains COVID-positive individuals and their close contacts. That said, CTNs can be constructed in different ways from CT data, and they can be complex and large as people are mobile and may show up in various places at different times. We focus on CTNs constructed for a pre-defined population during a pre-specified period time (e.g., employees in an organization or students in a school in one day, 2 weeks, or 1 month, etc). For example, suppose the time period is one day, starting at noon on June 1 2020 ending at noon on the next day and the population is all students at a college. If a COVID-positive student named Tom was in a dining hall from noon to 1pm on June 1, 2020 and had 2 close contacts, at the library from 1:30pm to 5pm and had 1 close contact, and in his dorm from 5pm to noon next day and had 5 close contacts, then Tom and all his 8 close contacts are included in the CTN, along with 8 edges, representing the 8 close contacts. We consider privacy-preserving release of CTNs with relational information only in this study; releasing CTNs with nodal attributes (such as demographic information or location information) with privacy guarantees is a topic for future research.

5.1 Method

We examine a few approaches for releasing privacy-preserving CTNs and present one approach, DP-ERGM, in the main text and include the other two in the supplementary materials. DP-ERGM stands for Differentially Private network synthesis via Exponential Random Graph Model (Liu et al., 2022). The DP-ERGM procedure can be regarded as an application of the model-based differentially private synthesis (MODIPS) approach (Liu, 2022) to graph data with ERGM as the synthesis model. ERGMs are a family of popular statistical models for analyzing network data (Robins et al., 2007; Snijders et al., 2006). Denote by \mathbf{e} the adjacency matrix in a network ($e_{ij} = 1$ if an edge exists between node i and node j ,

$e_{ij} = 0$ otherwise). ERGMs model the conditional distribution of \mathbf{e} as

$$p(\mathbf{e}|\boldsymbol{\theta}) = \frac{\exp\{\boldsymbol{\theta}^T \mathbf{S}(\mathbf{e})\}}{K(\boldsymbol{\theta})} \text{ with } K(\boldsymbol{\theta}) = \sum_{\mathbf{e}'} \exp\{\boldsymbol{\theta}^T \mathbf{S}(\mathbf{e}')\}, \quad (7)$$

where $\mathbf{S}(\mathbf{e})$ is the summary statistics that characterize the network structure such as number of edges, degree distribution, edge-wise shared partnership, etc. $K(\boldsymbol{\theta})$ is the normalizing constant summed over all possible adjacency matrix \mathbf{e}' and is often analytically intractable unless in small networks. Inference of $\boldsymbol{\theta}$ is often based on approaches with approximate $K(\boldsymbol{\theta})$, such as the Monte Carlo maximum likelihood estimation (Geyer and Thompson, 1992; Hunter and Handcock, 2006). Eq (7) is a simplified ERGM as we deal with CTN without nodal attributes in this study. In general, \mathbf{S} may contain statistics not only constructed from \mathbf{e} but also nodal statistics for networks with nodal attributes.

The steps of a general DP-ERGM procedure are as follows. Given a ERGM (either specified prior to the access to the observed data or chosen using a privacy-preserving procedure based on the observed by costing a portion of the total privacy budget), 1) derive the posterior distribution $\boldsymbol{\theta}$ given the likelihood function in Eq (7) and a prior on $\boldsymbol{\theta}$; 2) obtain a sanitized sample $\boldsymbol{\theta}^*$ from the posterior distribution with a pre-specified privacy budget ϵ ; 3) simulate a network \mathbf{e}^* via the ERGM parameterized by $\boldsymbol{\theta}^*$. If multiple sanitized networks are to be released, the above steps are repeated for $m > 1$ times.

In addition to DP-ERGM, we also examined a random response (RR) mechanism for perturbing edge information with DP guarantees (Karwa et al., 2017) and a debiased version of the RR mechanism (Liu et al., 2022). Both procedures perform significantly worse than the DP-ERGM procedure in the utility analysis performed in Section 5.2 unless the privacy loss is high ($\epsilon > 5$). The details on RR and RR-debias can be found in the supplementary materials.

5.2 Simulation Study

To evaluate statistical utility of sanitized CTNs, we conduct a simulation study. We simulated 500 sets of networks from an ERGM model with a single covariate s (edge count). In each simulated network, there are 100 nodes. The networks were simulated to mimic real-life CTN (a CT dataset collected at the University of Notre Dame, USA, during the pandemic) in the degree distribution per individual. The real data are not shareable due to privacy and IRB reasons.

The ERGM used in the DP-ERGM procedure contains edge count as a single covariate. We applied an approach in Liu (2022) to draw a privacy-preserving posterior sample on θ and also sanitized the edge count via the Laplace mechanism, which has a sensitivity of 1 (flipping a relation between two nodes changes the edge count in a network by at most 1). We equally split the total privacy budget ϵ between drawing a posterior sample of θ and sanitizing the edge count given a network. Given the privacy-preserving sample of θ and the sanitized edge count, we generated a privacy-preserving CTN under the constraint that its edge count equals to the sanitized edge count. We examine $\epsilon = 5, 2, 1, 0.5$. The ERGM model fitting and network simulation were completed using R package `statnet` (Handcock et al., 2008). We conduct two utility analyses. In the first analysis, we examine the preservation of

qualitative information and descriptive statistics in sanitized CTNs; in the second analysis, we run the ERGM on sanitized networks to examine the inference on the model parameter. m is set at 1 and 3, respectively, in these two analyses.

For the first utility analysis, we calculate some common network summary statistics, including edge counts, triangle counts, degree distribution (DD), and edgewise shared partners distribution (ESPD), and two node centrality measures in a sanitized network. Edge and triangle counts are the number of edges and triangles in a network. The DD in a network with n nodes consists of d_k for $k=0, \dots, n-1$, where d_k is the number of nodes that share an edge with exactly k other nodes. The ESPD consists of $\text{esp}_k/\text{edge count}$ for $k=1, \dots, \leq n(n-1)/2$, where esp_k is the number of edges whose two nodes are both connected with exactly k other nodes than themselves. The betweenness centrality measures the centrality of a node in a graph and is defined for node i as the proportion of the shortest paths that connect nodes j and j' while passing through node i ($j \neq j' \neq i$) among all shortest paths that connect nodes j and j' . There are multiple definitions of closeness centrality and we use $(\frac{A_i}{n-1})^2/C_i$, where A_i is the number of reachable nodes from node i , and C_i is the sum of distances from node i to all reachable nodes. If no nodes are connected with node i , its closeness centrality is 0.

The visualization of a single sanitized CTN from one of the 500 repeats are presented in Figure 5(a) and provides a big-picture comparison between the sanitized vs the original networks in terms of density, clustering, etc. In summary, the density of the sanitized CTNs via DP-ERGM is similar to the original CTN at all the examined ϵ values. Note the nodes in the sanitized networks do not match the nodes in the original CTN as DP-ERGM samples a whole new surrogate network from a differentially private ERGM model for release. The edge and triangles counts of the original networks are 39 and 10, respectively. The average (standard deviation) edge counts over 100 sanitized CTNs are 38 (6.4), 39 (3.1), 39 (1.4), and 39 (0.7) at $\epsilon = 0.5, 1, 2$, and 5, respectively; the average (standard deviation) triangle counts over 100 sanitized CTNs are 13 (9.2), 12 (7.4), 11 (6.8), and 11 (7.1) at $\epsilon = 0.5, 1, 2$, and 5, respectively. These numbers are consistent with the observations in Figure 5(a). Figures 5(b) and 5(c) depict the DD and ESPD of the sanitized CTN. In the latter, we also calculate the total variance distance (TVD) in ESPD between the sanitized and original CTNs, which are presented in Figure 5(c). Figures 5(d) and 5(e) show the box plots of the betweenness centrality and closeness centrality of the 100 nodes in the original and sanitized CTNs. Though there is some deviation in the DD, ESPD, and the distributions of the centrality measures in the sanitized CTNs from the original, the deviation is rather mild. In addition, the statistics are relatively stable across ϵ .

For the second utility analysis, we fitted the ERGM on the sanitized CTNs to obtain privacy-preserving inference on θ , the coefficient associated with edge count in ERGM, via the inferential rule in Eqs (5) and (6). The results are presented in Table 5. In summary, the results are acceptable for the ERGM analysis at all examined ϵ (especially for CP).

5.3 Summary

The simulation study suggests that the DP-ERGM approach can produce privacy-preserving CTNs that are structurally similar to original CTNs by various statistical measures. In

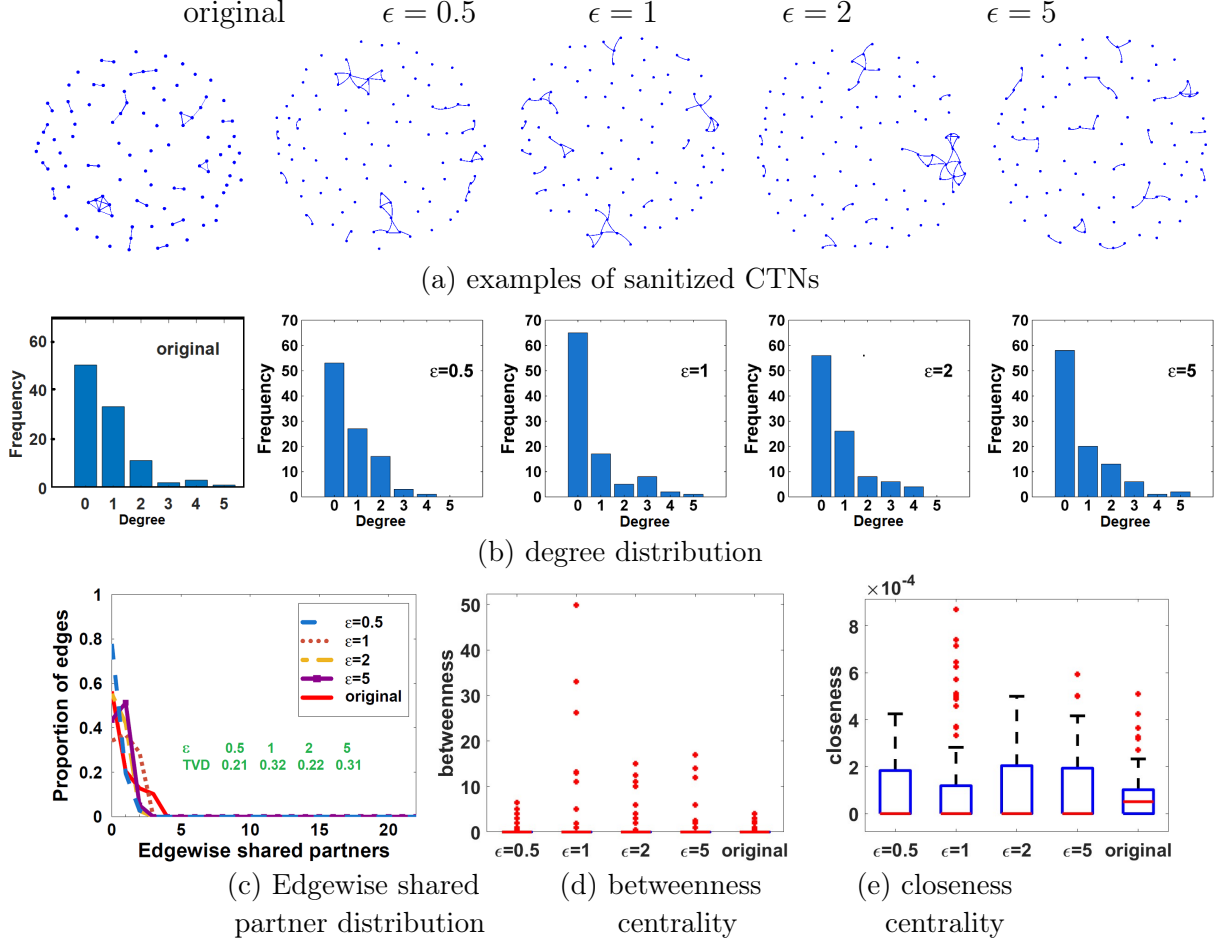


Figure 5: Comparison between the original and sanitized CTNs via DP-ERGM on various network structural statistics

Table 5: Inference of ERGM parameter based on sanitized CTNs ($m = 3, 500$ repeats)

	original [†]	$\epsilon = 5$	$\epsilon = 2$	$\epsilon = 1$	$\epsilon = 0.5$
bias	-0.021	-0.021	-0.026	-0.031	-0.051
RMSE	0.171	0.172	0.174	0.187	0.260
CP	0.942	0.954	0.954	0.952	0.944

addition, the utility of sanitized CTNs is relatively insensitive to ϵ for the examined range of $[0.5, 5]$, implying that a small ϵ can be used to provide strong privacy guarantees without sacrificing much of the utility. The sanitized CTNs can be shared with researchers who are interested in learning more about CTNs during the pandemic, without compromising individual privacy at a pre-specified privacy cost.

6 Discussion

We use three common data types – surveillance case numbers, case location information, and contact tracing networks – collected during the COVID-19 pandemic to demonstrate the release and sharing privacy-preserving data. In each data case, we apply randomized mechanisms with formal privacy guarantees to sanitize and release information aiming at preservation of statistical utility and aggregate information that can be used to infer under-

lying population parameters, as shown in the simulation studies and real-life applications. The approaches do not target at learning individual-level information, which not only conflicts with the goal of privacy protection, but is also unnecessary for the purposes of mining and understanding the population-level information.

DP and its various extensions are state-of-the-art concepts in privacy research and are quickly adopted in practice. Some of the methods we have demonstrated in the study are basic and have been routinely applied for privacy protection, such as the flat sanitizer; and some are recently proposed, such as DP-ERGM. For all the data types and examples examined in this study, synthetic data are generated and released at a pre-specified privacy budget and users may perform their own analysis on the synthetic data without having to worry about additional privacy loss. Our simulation studies suggest that different DP methods may lead to different utility and vary in the easiness of implementation for a given statistical analysis procedure at the same privacy cost, an observation that is well documented in the literature and also one of the reasons why new DP methods are constantly proposed to improve on the existing methods with either better utility or more straightforward implementation. In addition, absolute privacy protection for individuals in a dataset only exists on paper unless the released information is completely random or independent of the dataset. In reality, there is always some loss in privacy when releasing new and useful information; larger privacy loss parameters means sacrifice in privacy in hope for better utility in released information. Choice of a proper privacy loss is a key step when implementing DP procedures.

We hope our study and the examples shed light on privacy-preserving sharing of COVID-19 data to help promote and encourage more data sharing for research use. For future work on this topic, we will continue to develop methods to deal with more complicated COVID-19 data sharing situations, such as releasing travel trajectories of COVID-19 patients, longitudinal data, and dynamic CTNs, CTNs with nodal attributes, among others.

References

- 5Lab. Covid-19 news tracker-location-based news about covid-19 in thailand. https://covidtracker.5lab.co/zh-hans?fbclid=IwAR1bAH4qDAZtWkdh2MVwAiFmow91AtRFg78-vPSZKr76__ezADD1BNwYHTyk, 2020. accessed on 5/17/2020.
- Martin Abadi, Andy Chu, Ian Goodfellow, H Brendan McMahan, Ilya Mironov, Kunal Talwar, and Li Zhang. Deep learning with differential privacy. In *Proceedings of the 2016 ACM SIGSAC conference on computer and communications security*, pages 308–318, 2016.
- Ahmet Aktay, Shailesh Bavadekar, Gwen Cossoul, John Davis, Damien Desfontaines, Alex Fabrikant, Evgeniy Gabrilovich, Krishna Gadepalli, Bryant Gipson, Miguel Guevara, et al. Google covid-19 community mobility reports: Anonymization process description (version 1.0). *arXiv:2004.04145*, 2020.
- Miguel E Andrés, Nicolás E Bordenabe, Konstantinos Chatzikokolakis, and Catuscia Palamidessi. Geo-indistinguishability: Differential privacy for location-based systems. In *Proceedings of the 2013 ACM SIGSAC conference on Computer & communications security*, pages 901–914, 2013.

- Apple. Apple differential privacy technical overview. https://www.apple.com/privacy/docs/Differential_Privacy_Overview.pdf, 2020. accessed on 6/13/2021.
- Apple and Google. Privacy-preserving contact tracing. <https://covid19.apple.com/contacttracing/>, 2020. accessed on 5/23/2021.
- Adrian Baddeley and Rolf Turner. Spatstat: an r package for analyzing spatial point patterns. *Journal of statistical software*, 12:1–42, 2005.
- Claire McKay Bowen and Fang Liu. Comparative study of differentially private data synthesis methods. *Statistical Science*, 35(2):280–307, 2020.
- Claire McKay Bowen, Fang Liu, and Bingyue Su. Differentially private data release via statistical election to partition sequentially. *METRON*, 79(1):1–31, 2021.
- Mark Bun and Thomas Steinke. Concentrated differential privacy: Simplifications, extensions, and lower bounds. In *Theory of Cryptography Conference*, pages 635–658, 2016.
- US Census Bureau. Census bureau sets key parameters to protect privacy in 2020 census results. <https://fwww.census.gov/newsroom/press-releases/2021/2020-census-key-parameters.html>, 2020. accessed on 6/13/2021.
- David Butler, Chris Hicks, James Bell, Carsten Maple, and Jon Crowcroft. Differentially private health tokens for estimating covid-19 risk. *arXiv:2006.14329*, 2020.
- CDC. location history. <https://www.cdc.gov/coronavirus/2019-ncov/php/contact-tracing/keyinfo.html>, 2021. accessed on 5/11/2021.
- Kamalika Chaudhuri, Claire Monteleoni, and Anand D Sarwate. Differentially private empirical risk minimization. *Journal of Machine Learning Research*, 12(3), 2011.
- Jinshuo Dong, Aaron Roth, and Weijie Su. Gaussian differential privacy. *Journal of the Royal Statistical Society*, 2021.
- John C Duchi, Michael I Jordan, and Martin J Wainwright. Local privacy and statistical minimax rates. In *2013 IEEE 54th Annual Symposium on Foundations of Computer Science*, pages 429–438, 2013.
- Cynthia Dwork and Aaron Roth. The algorithmic foundations of differential privacy. *Foundations and Trends in Theoretical Computer Science*, 9(3-4):211–407, 2014.
- Cynthia Dwork and Guy N. Rothblum. Concentrated differential privacy. *arXiv:1603.01887v2*, 2016.
- Cynthia Dwork, Krishnaram Kenthapadi, Frank McSherry, Ilya Mironov, and Moni Naor. Our data, ourselves: Privacy via distributed noise generation. In *Annual International Conference on the Theory and Applications of Cryptographic Techniques*, pages 486–503, 2006a.
- Cynthia Dwork, Frank McSherry, Kobbi Nissim, and Adam Smith. Calibrating noise to sensitivity in private data analysis. In *Theory of cryptography conference*, pages 265–284, 2006b.
- Cynthia Dwork, Guy N Rothblum, and Salil Vadhan. Boosting and differential privacy. In *2010 IEEE 51st Annual Symposium on Foundations of Computer Science*, pages 51–60, 2010.

- Cynthia Dwork, Nitin Kohli, and Deirdre Mulligan. Differential privacy in practice: Expose your epsilons! *Journal of Privacy and Confidentiality*, 9(2), 2019.
- Evercita Eugenio and Fang Liu. Construction of differentially private empirical distributions from a low-order marginals set through solving linear equations with l2 regularization. In *Intelligent Computing, Proceedings of the 2021 Computing Conference*, volume 3, pages 949–966. Springer, 2021.
- Alex Fabrikant, Andrew Mingbo Dai, Chaitanya Kamath, Charlotte Stanton, Damien Desfontaines, Dennis Kraft, Evgeniy Gabrilovich, Gerardo Flores, Gregory Alexander Welle-nius, Ilya Eckstein, et al. Google covid-19 search trends symptoms dataset: Anonymization process description. *arXiv:2009.01265v1*, 2020.
- Magdalena Gad-Nowak and Malgorzata P. Grzelak. Covid-19: Poland launches an official tracking app. <https://www.natlawreview.com/article/covid-19-poland-launches-official-tracking-app>, 2020. accessed on 5/17/2020.
- Quan Geng and Pramod Viswanath. Optimal noise adding mechanisms for approximate differential privacy. *IEEE Transactions on Information Theory*, 62(2):952–969, 2015.
- C. J. Geyer and E. A. Thompson. Constrained monte carlo maximum likelihood for dependent data. *Journal of the Royal Statistical Society, Series B*, 54:657–699, 1992.
- Shirin Ghaffary. What the us can learn from other countries using phones to track covid-19. <https://www.vox.com/recode/2020/4/18/21224178/covid-19-tech-tracking-phones-china-singapore-taiwan-korea-google-apple-contact-tracing-digital>, 2020. accessed on 5/14/2020.
- Mark S Handcock, David R Hunter, Carter T Butts, Steven M Goodreau, and Martina Morris. statnet: Software tools for the representation, visualization, analysis and simulation of network data. *Journal of statistical software*, 24(1):1548, 2008.
- Michael Hay, Vibhor Rastogi, Gerome Miklau, and Dan Suciu. Boosting the accuracy of differentially private histograms through consistency. *Proceedings of the VLDB Endowment*, 3(1-2):1021–1032, 2010.
- D. Hunter and M. Handcock. Inference in curved exponential family models for network. *Journal of Computational and Graphical Statistics*, 15:565–583, 2006.
- Amol Kapoor, Xue Ben, Luyang Liu, Bryan Perozzi, Matt Barnes, Martin Blais, and Shawn O’Banion. Examining covid-19 forecasting using spatio-temporal graph neural networks. *arXiv:2007.03113*, 2020.
- Vishesh Karwa, Pavel N Krivitsky, and Aleksandra B Slavković. Sharing social network data: differentially private estimation of exponential family random-graph models. *Journal of the Royal Statistical Society: Series C (Applied Statistics)*, 66(3):481–500, 2017.
- Daniel Kifer and Ashwin Machanavajjhala. No free lunch in data privacy. In *Proceedings of the 2011 ACM SIGMOD International Conference on Management of Data*, page 193–204, 2011.
- Daniel Kifer, Adam Smith, and Abhradeep Thakurta. Private convex empirical risk minimization and high-dimensional regression. In *Conference on Learning Theory*, pages 25–1. JMLR Workshop and Conference Proceedings, 2012.

- Bai Li, Vishesh Karwa, Aleksandra Slavković, and Rebecca Carter Steorts. A privacy preserving algorithm to release sparse high-dimensional histograms. *Journal of Privacy and Confidentiality*, 8(1), 2018.
- Yinan Li and Fang Liu. Noise-augmented privacy-preserving empirical risk minimization with dual-purpose regularizer and privacy budget retrieval and recycling. In *Intelligent Computing*, pages 660–681, Cham, 2022. Springer International Publishing.
- Fang Liu. Generalized Gaussian mechanism for differential privacy. *IEEE Transactions on Knowledge and Data Engineering*, 31(4):747–756, 2018.
- Fang Liu. Statistical properties of sanitized results from differentially private laplace mechanism with univariate bounding constraints. *Transactions on Data Privacy*, 12(3):169 – 195, 2019.
- Fang Liu. Model-based differentially private data synthesis and statistical inference in multiply synthetic differentially private data. *Transactions on Data Privacy*, 15(3), 2022.
- Fang Liu, Dong Wang, and Zheng-Quan Xu. Privacy-preserving travel time prediction with uncertainty using gps trace data. *IEEE Transactions on Mobile Computing* (DOI:10.1109/TMC.2021.3074865), 2021.
- Fang Liu, Evercita C. Eugenio, Ick Hoon Jin, and Claire Bowen. Differentially private synthesis and sharing of network data via bayesian exponential random graph models. *Journal of Survey Statistics and Methodology*, 10:2, 2022.
- Ashwin Machanavajjhala, Daniel Kifer, John Abowd, Johannes Gehrke, and Lars Vilhuber. Privacy: Theory meets practice on the map. In *2008 IEEE 24th international conference on data engineering*, pages 277–286, 2008.
- Frank McSherry and Kunal Talwar. Mechanism design via differential privacy. In *48th Annual IEEE Symposium on Foundations of Computer Science (FOCS’07)*, pages 94–103, 2007.
- Ilya Mironov. Rényi differential privacy. In *2017 IEEE 30th Computer Security Foundations Symposium (CSF)*, pages 263–275, 2017.
- Zümrüt Müftüoğlu, M Ayyüce Kizrak, and Tülay Yildırım. Differential privacy practice on diagnosis of covid-19 radiology imaging using efficientnet. In *2020 International Conference on INnovations in Intelligent SysTems and Applications (INISTA)*, pages 1–6, 2020.
- National Health Commission of China. Location privacy. <https://baijiahao.baidu.com/s?id=1685656325236477831&wfr=spider&for=pc>, 2021a. accessed on 5/11/2021.
- National Health Commission of China. publish location information. <https://baijiahao.baidu.com/s?id=1688551020040753847&wfr=spider&for=pc>, 2021b. accessed on 5/11/2021.
- European Parliament. Use of smartphone data to manage covid-19 must respect eu data protection rules. <https://www.europarl.europa.eu/news/en/press-room/20200406IPR76604/use-of-smartphone-data-to-manage-covid-19-must-respect-eu-data-protection-rules>, 2020. accessed on 5/13/2020.
- Ramesh Raskar, Sandy Pentland, Kent Larson, and Kevin Esvelt. Safe path. <http://safepaths.mit.edu/>, 2020. accessed on 5/17/2020.

- G. Robins, T. Snijders, P. Wang, M. Handcock, and P. Pattison. Recent development in exponential random graph models for social networks. *Social Networks*, 29:192–215, 2007.
- T. A. B. Snijders, P. E. Pattison, G. L. Robins, and M. S. Handcock. New specification for exponential random graph models. *Sociological Methodology*, 36:99–153, 2006.
- Anwaar Ulhaq and Oliver Burmeister. Covid-19 imaging data privacy by federated learning design: A theoretical framework. *arXiv:2010.06177*, 2020.
- Dong Wang and Fang Liu. Privacy risk and preservation in contact tracing of covid-19. *Chance*, 33(3):49–55, 2020.
- Gregory A Wellenius, S Vispute, V Espinosa, A Fabrikant, TC Tsai, J Hennessy, A Dai, B Williams, K Gadepalli, A Boulanger, et al. Impacts of social distancing policies on mobility and covid-19 case growth in the us. *Nature Communications*, 12, 2021.
- Sarah Wray. South korea to step-up online coronavirus tracking. <https://www.smartcitiesworld.net/news/news/south-korea-to-step-up-online-coronavirus-tracking-5109>, 2020. accessed on 5/14/2020.
- Xiaokui Xiao, Gabriel Bender, Michael Hay, and Johannes Gehrke. ireduct: Differential privacy with reduced relative errors. In *Proceedings of the 2011 ACM SIGMOD International Conference on Management of data*, pages 229–240, 2011.
- Yonghui Xiao, James Gardner, and Li Xiong. Dpcube: Releasing differentially private data cubes for health information. In *2012 IEEE 28th International Conference on Data Engineering*, pages 1305–1308, 2012.
- Jia Xu, Zhenjie Zhang, Xiaokui Xiao, Yin Yang, Ge Yu, and Marianne Winslett. Differentially private histogram publication. *The VLDB Journal*, 22(6):797–822, 2013.
- Xiaojian Zhang, Rui Chen, Jianliang Xu, Xiaofeng Meng, and Yingtao Xie. Towards accurate histogram publication under differential privacy. In *Proceedings of the 2014 SIAM international conference on data mining*, pages 587–595, 2014.

Supplementary Materials to “*Some Examples of Privacy-preserving Publication and Sharing of COVID-19 Pandemic Data*”

UH and UHp for Surveillance Case Number Release

The UH approach forms a hierarchical tree among the data attributes and injects noise to each the node count in each layer of the tree, explores equality constraints between each parent node and its children nodes in the tree to improve the accuracy of the sanitized count of the parent nodes (low-order marginals) and release the final corrected counts from the whole tree. Figure S1 displays a 4-layer hierarchical tree formed in the UH approach on a data set with 3 variables (age group, minority/majority, sex). We refer to the node at the top of the tree as the root (layer 1) and those at the bottom as the leaf nodes (layer 4). The age nodes at layer 3 are parents to the race/ethnicity nodes in layer 3, which are the parent nodes to the sex nodes in layer 4. There is no particular ordering among the three attributes in the example in Figure S1. We can place the attributes in the middle layers of the trees that would enjoy a lower mean squared error (MSE) (MSE for a sanitized count \tilde{x} is $\mathbb{E}_{\mathcal{M}}(\tilde{x} - x)^2$, where x is the original count and the expectation is taken over the distribution of the randomized algorithm). in their marginal sanitized counts relative to their original counts, compared to the MSE resulting from a simple sum of the directly sanitized counts of the most granular cells as done in the flat sanitizer.

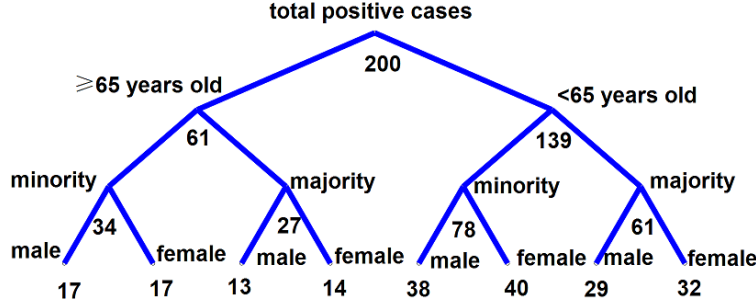


Figure S1: A count hierarchical tree with three binary attributes

The UH procedure is implemented in 3 steps. First, since each layer is sanitized, the total budget ϵ should be split among the layers following the sequential composition principle in DP (McSherry and Talwar, 2007). For illustration purposes, we assume each layer receives $1/l$ of the total ϵ , where l is the height of the tree (other privacy allocation schemes across the layers can also be used). and $l = 4$ in Example 1. The count $h[v]$ in each node v in the tree is sanitized via the Laplace mechanism $\text{Lap}(0, l\epsilon^{-1})$; that is, $\tilde{h}[v] = h[v] + e$, where $e \sim \text{Lap}(l\epsilon^{-1})$, where $\tilde{h}[v]$ is the sanitized count. In step 2, intermediate node count $z[v]$ for each node v is obtained via Eq (S1),

$$z[v] = \begin{cases} \tilde{h}[v], & \text{if } v \text{ is the leaf node} \\ \frac{k^l - k^{l-1}}{k^l - 1} \tilde{h}[v] + \frac{k^{l-1} - 1}{k^l - 1} \sum_{u \in \text{succ}(v)} z[u], & \text{o.w.} \end{cases}, \quad (\text{S1})$$

where $\text{succ}(v)$ denotes the set of children nodes to parent node v and k is the number of children per parent node, which is assumed to be the same for each parent ($k = 2$ in example 1). The reason behind Eq (S1) is that for the nodes not from the bottom layer (the non-leaf nodes), a sanitized count comes from two sources (the node being sanitized, and the summation from its children nodes) so Eq (S1) calculates a weighted average of the two. Obviously, $z[v]$ may no longer equal to the sum of the node counts of its children nodes, violating the equality constraints in contingency tables. This inconsistency is corrected via Eq (S2), yielding the final sanitized count $h^*[v]$

$$h^*[v] = \begin{cases} z[v] & \text{if } v \text{ is the root node} \\ z[v] + k^{-1} \left(h^*[u] - \sum_{w \in \text{succ}(u)} z[w] \right), & \text{o.w.} \end{cases}, \quad (\text{S2})$$

where u is the parent node to node v , $\text{succ}(u)$ contains the children nodes to parent node u , and $h^*[u] - \sum_{w \in \text{succ}(u)} z[w]$ is the correction term to ensure the equality constraint holds for each parent node in the tree.

We extend the UH approach to sanitizing a proportion tree (Figure S1) in place of a count tree and name it the UHp approach (“p” in the name “UH_p” stands for “proportion”), in cases where the total sample size n is public information and can be released directly, or when it is desirable not to alter n from a statistical inferential perspective as n is critical for inferences such as inferential efficiency.

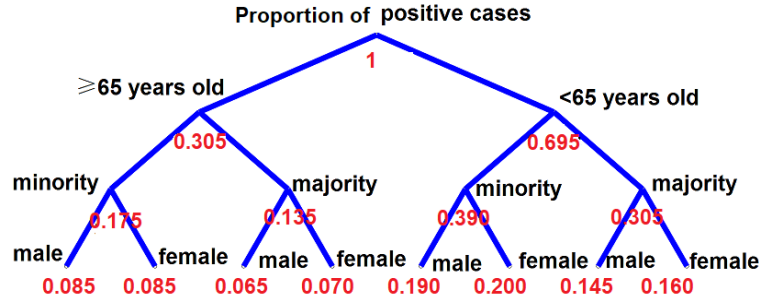


Figure S2: A proportion hierarchical tree with three binary attributes

The sanitization process for UHp is similar to UH with a few modifications. First, given the proportion at the top layer is always 1, there is no need to sanitize the node and the total ϵ is only needed to split into $l - 1$ layers. Second, the Laplace distribution from which the noise is drawn becomes $\text{Laplace}(0, (l - 1)\epsilon^{-1}/n)$ as the global sensitivity for proportion is $1/n$. Third, after obtaining $\tilde{h}[v] = h[v] + e$, where $e \sim \text{Lap}((l - 1)\epsilon^{-1}/n)$ for all the non-root node proportions, we normalize the proportions in layer 2 as in $\tilde{h}[v^{(2)}] = \tilde{h}[v^{(2)}] / \sum_u \tilde{h}[u]$, where u refers to all the nodes in layer 2, so that the layer-2 proportions sum up to 1, honoring the constraint of $\tilde{h}[v] = h[v] = 1$ for the root node. The steps in Eqs (S1) and (S2) after the normalization step remain the same as in the UH approach. After the sanitized proportions are obtained, the corresponding counts can be obtained by multiplying the proportions with the total n .

Similar to the flat sanitizer, the sanitized counts or proportions in the UH and the UHp approaches can be negative as the support of the Laplace distribution is \mathbb{R} . In addition,

the sanitized proportions may be > 1 . We applied the same methods as used for the flat sanitizer to deal with negative counts and in the case of a fixed upper bound such as the proportions add up to 1 and when the total count is fixed.

Simulation study and CDC death count application for UH and UHp

In the simulation study, for both UH and UHp, the tree height is $l = 4$ as there are 3 attributes – X_1 is layer 2, X_2 in layer 3, and X_3 in layer 4 – and $k = 2$ as all attributes are binary. The simulation results are presented in Figure S3, together with the flat Laplace sanitizer and the original results for comparison.

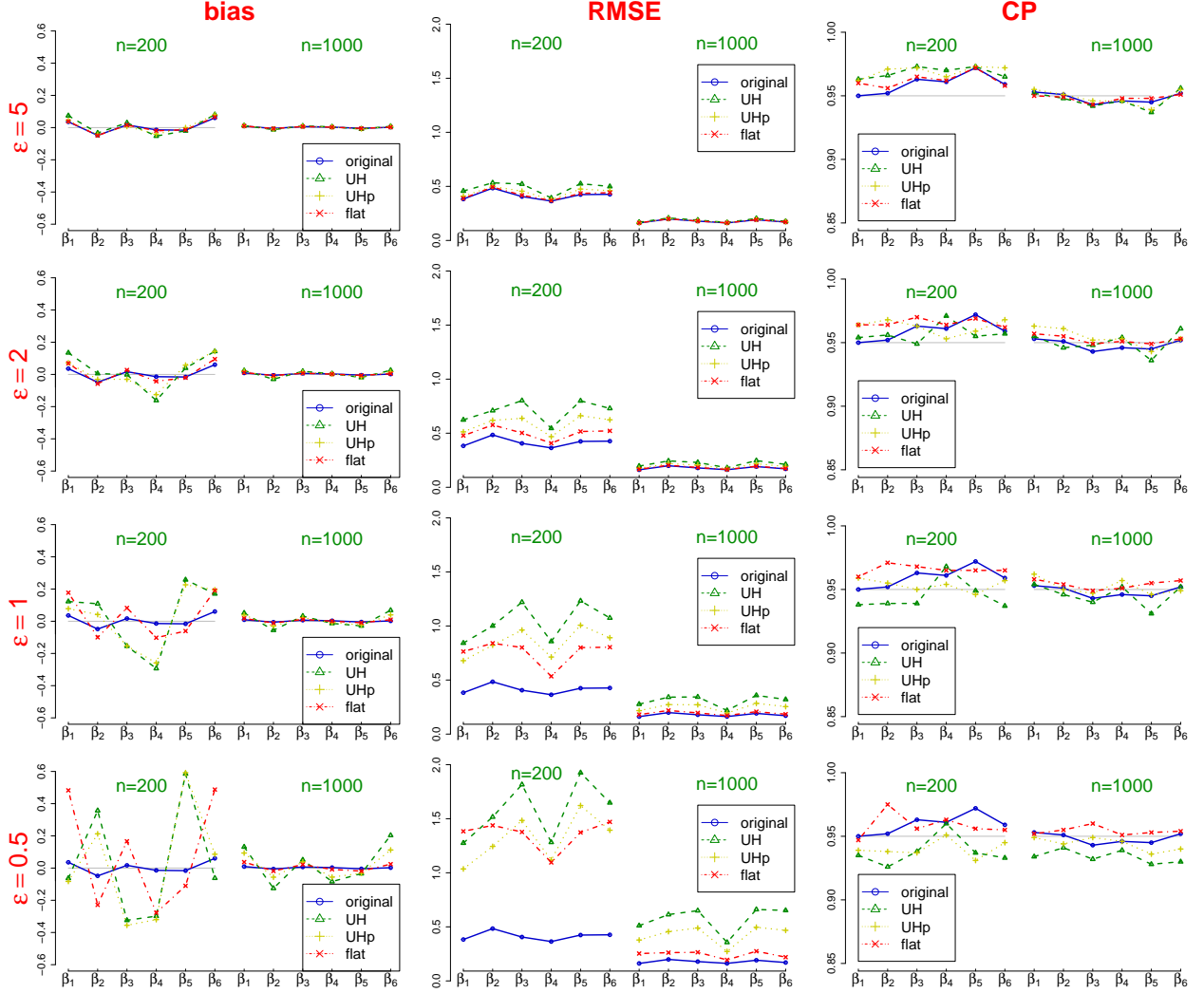


Figure S3: Privacy-preserving inference of the log-linear model based on sanitized counts by different methods in the simulation study ($m = 3, 500$ repeats)

For the application to the CDC COVID-19 death count data, $l = 3$ and $k = 7$ in the hierarchical tree for both UH and UHp. We placed age in layer 2 and race/ethnicity in layer 3 and don't expect the ordering would affect the results of the analysis we conducted in a statistically meaningful way. The results are presented in Figure S4, together with the flat Laplace sanitizer and the original results for comparison.

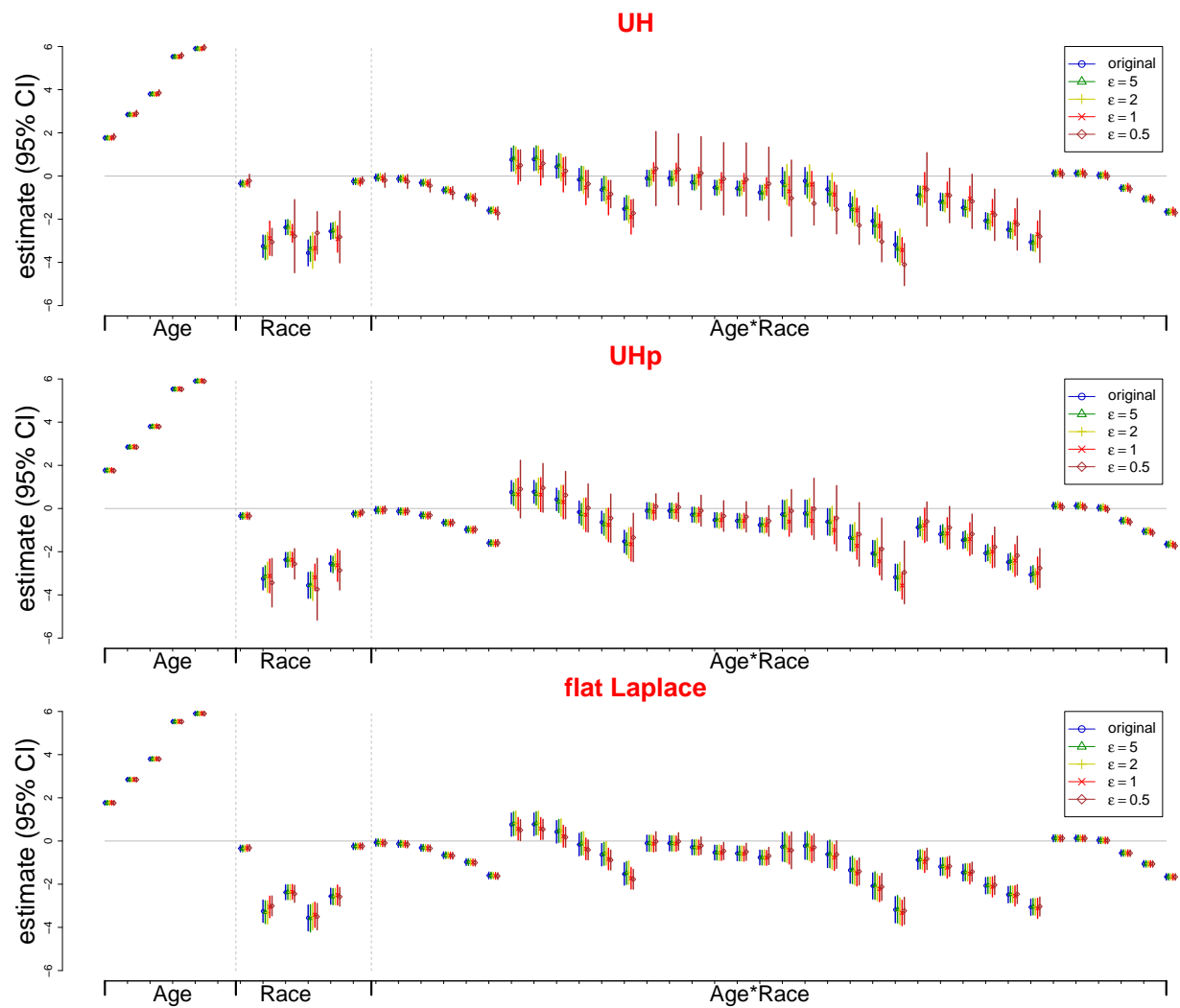


Figure S4: Privacy-Preserving results from the Log-linear model fitted on the CDC COVID-19 death data

Examples of sanitized US COVID-19 death counts by the Flat Laplace sanitizer ($m = 3$ and $\epsilon = 0.5$)

Table S1: Three sets of sanitized U.S. COVID-19 death counts by age group and race/ethnicity on May 24, 2022 ($m = 3, \epsilon = 0.5$) by the flat Laplace sanitizer

Age (ys)	Race/Ethnicity							Total
group	NH White	NH Black	NH AIAN	NH Asian	NH NHPI	NH Mix	Hispanic	
<17	385	273	19	38	14	25	302	1056
18-29	2265	1480	183	181	33	78	2018	6238
30-39	6665	4140	570	561	151	160	5916	18162
40-49	17277	8939	1024	1200	267	313	13979	43000
50-64	97407	35752	3196	5310	703	955	43655	186979
65-74	141417	37760	2913	7431	498	914	38416	229350
>75	380635	54588	3210	16515	447	1383	56700	513478
Total	646051	142933	11115	31236	2114	3827	160986	998262

Age (ys)	Race/Ethnicity							Total
group	NH White	NH Black	NH AIAN	NH Asian	NH NHPI	NH Mix	Hispanic	
<17	387	289	19	34	11	35	304	1079
18-29	2273	1492	183	197	54	86	2014	6299
30-39	6660	4124	568	571	147	157	5917	18145
40-49	17269	8930	1029	1216	279	314	13972	43010
50-64	97386	35756	3200	5315	723	953	43647	186982
65-74	141407	37753	2890	7426	513	918	38420	229327
>75	380591	54568	3205	16518	450	1382	56706	513420
Total	645974	142912	11095	31278	2177	3846	160980	998262

Age (ys)	Race/Ethnicity							Total
group	NH White	NH Black	NH AIAN	NH Asian	NH NHPI	NH Mix	Hispanic	
<17	392	284	19	29	10	29	309	1072
18-29	2236	1507	189	196	48	62	2007	6243
30-39	6659	4146	563	562	150	153	5903	18135
40-49	17260	8933	1002	1208	287	316	13983	42987
50-64	97418	35743	3198	5312	719	964	43674	187027
65-74	141398	37767	2897	7437	516	903	38420	229339
>75	380604	54573	3192	16513	460	1391	56724	513458
Total	645966	142953	11060	31255	2190	3818	161020	998262

Race/ethnicity = 'unknown' is not included in the table.

NH = Non-Hispanic; AIAN = American Indian or Alaska Native; NHPI = Native Hawaiian or Other Pacific Islander; "Mix" means "more than one race"

The RR mechanism and the RR-debiased procedure

The RR mechanism for sanitizing edges in a network works as follows. Let p_{ij} denote the probability the original edge $e_{ij} = 1$ is retained and q_{ij} be the probability that $e_{ij} = 0$ is retained after sanitization for nodes $i \neq j = 1, \dots, n$. To satisfy ϵ_{ij} -DP (ϵ_{ij} edge DP precisely speaking; see Liu et al. (2022) for details) in the sanitization of the relational information $e_{ij} = 1$, one may set $p_{ij} = q_{ij} = e^{\epsilon_{ij}}/(1 + e^{\epsilon_{ij}})$. When there is no particular reasons for using different ϵ_{ij} for different pairs of nodes, one may set $\epsilon_{ij} \equiv \epsilon$ and the probability of edge flipping in the network is

$$p_{ij} = q_{ij} \equiv 1/(1 + e^\epsilon). \quad (\text{S3})$$

If all edges are mutually independent, the total cost for sanitizing the whole network is also ϵ per the parallel composition principle.

Liu et al. (2022) employs a debiasing approach as an attempt to remove bias in sanitized networks via the RR mechanism (with edges e_{ij}^*) by synthesizing new networks with edges \tilde{e}_{ij}^* given a RR-sanitized network. Specifically,

$$\tilde{e}_{ij}^* | e_{ij}^* = 1 \sim \text{Bern}(p_1), \text{ where } p_1 = \frac{(p + q - 1)q}{(2q - 1)p}, \quad (\text{S4})$$

$$\tilde{e}_{ij}^* | e_{ij}^* = 0 \sim \text{Bern}(p_0), \text{ where } p_0 = \frac{q(p + q - 1)}{(1 - p)(2q - 1)}, \quad (\text{S5})$$

where $q = e^\epsilon/(1 + e^\epsilon)$ is the probability of retaining an original edge by RR and p is the proportion of all $e_{ij}^* = 1$ in row i of the adjacency matrix of the synthetic network generated by RR (without the diagonal element), and. Synthetic networks via RR-debiased can be summarized and analyzed in the same way as the original network including descriptive statistics, visualization, and inference. For inference, there is no need to explicitly model the RR mechanism or the subsequent debiasing/sanitization process if $m > 1$ sets of synthetic networks are released. The debiasing procedure does not use the information from the original network and thus maintains the privacy guarantees, but at the cost of introducing another layer of variability. The debiased sanitized network is made of edges Y^* drawn from two Bernoulli distributions, depending on whether the synthetic edge Y' from the DWRR is 1 or 0.

Simulation Study on RR and RR-debiased

For RR, the probability of flipping an edge per Eq (S3) is $(1 + e^5)^{-1} = 0.7\%$, $(1 + e^2)^{-1} = 11.9\%$, $(1 + e)^{-1} = 26.9\%$ and $(1 + e^{0.5})^{-1} = 37.5\%$ at $\epsilon = 5, 2, 1, 0.5$, respectively. Though the probability retaining the original relation between nodes i and j is very low at $\epsilon = 5$, but the number of edges is expected to double $(39e^5/(1 + e^5) + (4950 - 39)e^5/(1 + e^5) = 71.6$ where 39 is the edge count in the original network).

The sanitized CTNs via RR and RR-debiased are presented in Figure S5 with the original CTN presented for comparison. Table S2 presents the number of edges and number of triangles of the sanitized CTNs via RR and RR-debias. Figure S6 shows the DD, which is the distribution of close contacts of an individual in a CTN via RR and RR-debias and Figures S7 depicts the ESPD of the sanitized CTNs with the TVD in DD between the

sanitized and original CTNs. Figure S8 shows the box plots of the betweenness centrality and closeness centrality of the 100 nodes in the sanitized CTNs via RR and RR-debias vs the original.

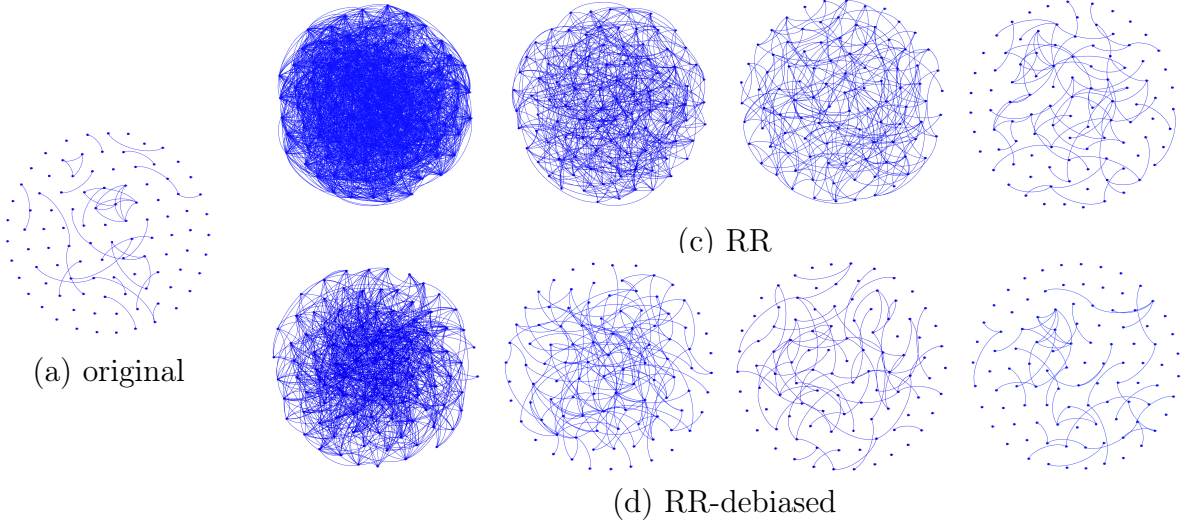


Figure S5: Examples of differentially privately sanitized CTNs via RR and RR-debiased

Table S2: Average (SD) number of edges and number of triangles over 100 repeats

ϵ	RR		RR-debiased	
	number of edges	number of triangle	number of edges	number of triangle
0.5	1876 (37.4)	8802 (528.3)	844 (82.4)	1258 (356.4)
2	619 (20.9)	320 (38.1)	182 (21.9)	14 (6.1)
5	72 (5.2)	10 (0.9)	48 (6.2)	6 (2.5)
8	40 (1.3)	10 (0.3)	40 (1.4)	9 (0.7)
10	39 (0.5)	10 (0.1)	39 (0.4)	10 (0)

original: number of edges = 39; number of triangle = 10.

The results on the privacy-preserving inference of the ERGM based on the sanitized CTNs via RR and RR-debias are presented in Table S3. We present the results for $\epsilon = 5, 15, 18, 24$; the results at $\epsilon < 5$ are even worse.

Table S3: Privacy-preserving Inference of β in the ERGM model based sanitized CTNs via RR and RR-debiased ($m = 3$; 500 repeats)

method	metric	$\epsilon = 5$	$\epsilon = 15$	$\epsilon = 18$	$\epsilon = 24$
RR	bias	3.260	0.627	0.269	0.023
	RMSE	3.260	0.635	0.299	0.165
	CP	0	0.002	0.366	0.832
RR-debiased	bias	1.500	0.305	0.147	0.008
	RMSE	1.501	0.330	0.204	0.165
	CP	0	0.366	0.704	0.830
Original data: bias = -0.021, RMSE = 0.171, and CP = 0.942.					

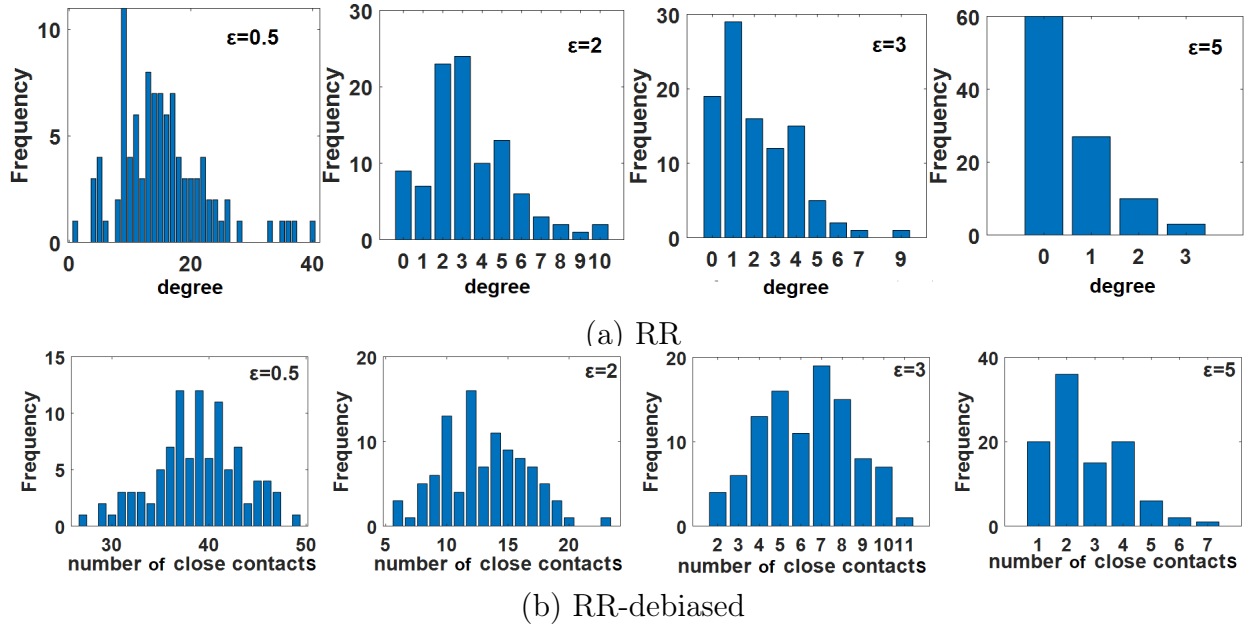


Figure S6: Degree distribution in the original and sanitized CTNs via RR and RR-debias

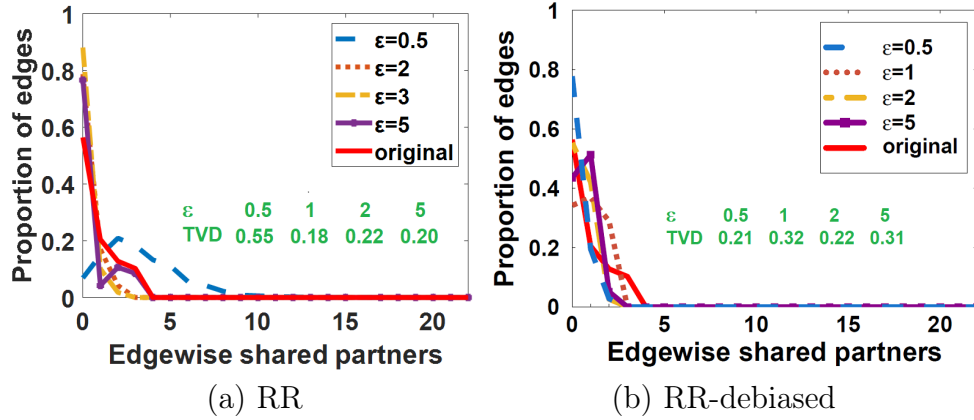


Figure S7: Edgewise shared partner distribution in sanitized CTNs via RR and RR-debias

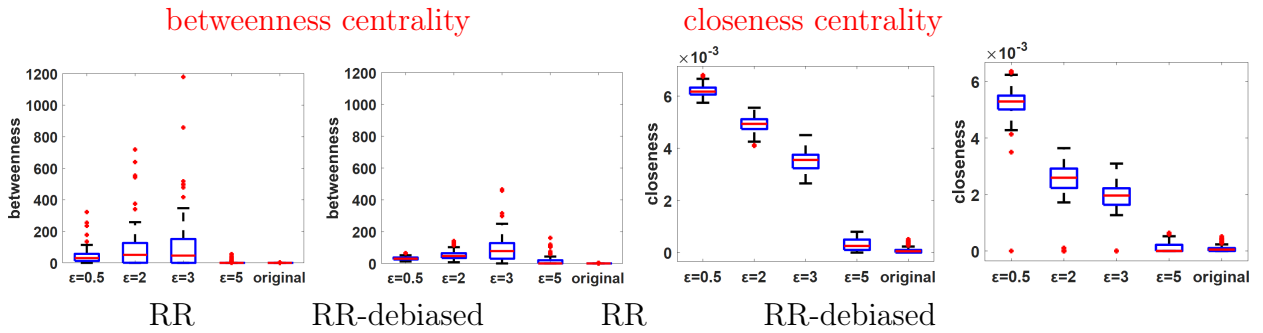


Figure S8: Box plots of betweenness centrality and closeness centrality of 100 nodes in original and sanitized CTNs via RR and RR-debias